International Telecommunication Union

ITU-R

Radiocommunication Sector of ITU

Report ITU-R BT.2142
(05/2009)

The effect of the scattering of digital television signals from a wind turbine

BT Series

Broadcasting service (television)

Foreword

The role of the Radiocommunication Sector is to ensure the rational, equitable, efficient and economical use of the radio-frequency spectrum by all radiocommunication services, including satellite services, and carry out studies without limit of frequency range on the basis of which Recommendations are adopted.

The regulatory and policy functions of the Radiocommunication Sector are performed by World and Regional Radiocommunication Conferences and Radiocommunication Assemblies supported by Study Groups.

Policy on Intellectual Property Right (IPR)

ITU-R policy on IPR is described in the Common Patent Policy for ITU-T/ITU-R/ISO/IEC referenced in Annex 1 of Resolution ITU-R 1. Forms to be used for the submission of patent statements and licensing declarations by patent holders are available from http://www.itu.int/ITU-R/go/patents/en where the Guidelines for Implementation of the Common Patent Policy for ITU-T/ITU-R/ISO/IEC and the ITU-R patent information database can also be found.

Series of ITU-R Reports

(Also available online at http://www.itu.int/publ/R-REP/en)

Series	Title
BO	Satellite delivery
BR	Recording for production, archival and play-out; film for television
BS	Broadcasting service (sound)
BT	**Broadcasting service (television)**
F	Fixed service
M	Mobile, radiodetermination, amateur and related satellite services
P	Radiowave propagation
RA	Radio astronomy
RS	Remote sensing systems
SA	Space applications and meteorology
SF	Frequency sharing and coordination between fixed-satellite and fixed service systems
SM	Spectrum management

Note: *This ITU-R Report was approved in English by the Study Group under the procedure detailed in Resolution ITU-R 1.*

Electronic Publication
Geneva, 2009

REPORT ITU-R BT.2142

The effect of the scattering of digital television signals from a wind turbine

(2009)

1 Introduction

This Report is on the topic of performance of television reception in the presence of reflected signals, specifically those from wind turbines as identified in the preliminary draft new Recommendation ITU-R [XXX] – Assessment of impairment caused to digital television reception by a wind turbine (Annex 2 to Document 6A/196).

It results from studies in Australia.

2 Background

Wind turbine farms are proving to be a popular energy source. Due to this growth many administrations are now experiencing interest from developers in constructing wind farms. This has raised concerns about the potential impact of wind farms on the reception of broadcasting services.

In considering the planning for digital television services within the VHF and UHF broadcasting bands traditionally used for analogue television services, some administrations have sought to reference Recommendation ITU-R BT.805 – Assessment of impairment caused to television reception by a wind turbine. Recommendation ITU-R BT.805 – was approved in 1992 in response to Question ITU-R 6/11. Preliminary draft new Recommendation ITU-R [XXX] – Assessment of impairment caused to digital television reception by a wind turbine has been developed to address the emergence of digital television and it retains the reference to the Question ITU-R 6/11. However, a current Question ITU-R 69/6 – Conditions for a satisfactory television service in the presence of reflected signals deals with reflections affecting analogue television systems.

In 2004 Australia proposed a draft modification to Question ITU-R 69/6 that extended studies to include digital television. The purpose was to encourage eventual modifications to Recommendation ITU-R BT.805 as a result of further study as to whether impairment is caused by wind turbines to digital television, as well as the development of further Recommendations, should they be required, relating to reflections from other objects.

In 2006 Australia proposed that a working document towards a modification of Recommendation ITU-R BT.805 be developed based on studies conducted in Australia. The study based on theoretical modelling identified that Recommendation ITU-R BT.805 is not adequate for predicting interference from wind farms for analogue and digital TV signals.

In 2007 a further study indicated that the methods to assist in quality assessment of the coverage and service area for digital television broadcasting in System B in Recommendation ITU-R BT.1735 are not satisfactory for the type of dynamic signal variations from rotating wind turbine blades.

From studies undertaken by Australia to date, Recommendation ITU-R BT.805 does not currently provide adequate advice for predicting interference from wind farms for analogue and digital TV signals. Subsequently Working Party 6A proposed a Preliminary draft new Recommendation ITU-R [XXX] – Assessment of impairment caused to digital television reception by a wind turbine be developed.

Australia also observed that further study is required to review the relationship between the mean MER, slow MER variations, short deep MER notches and the receiver performance.

The annexes to this Report contain the results of studies to date:

Annex 1 – Scattering model calculations.

Annex 2 – The effect of the scattering of digital television signals from wind turbines.

Annex 1

Scattering model calculations

1 Introduction

This annex analyses the scattering model used in Recommendation ITU-R BT.805, describes its limitations and weaknesses, and suggests improvements. The analysis is extended to include the scattering from rotating triangular shaped blades and the wind turbine pylon.

2 Analysis

2.1 Overview

The basis for the scattering model in Recommendation ITU-R BT.805 is somewhat unclear, as it apparently calculates backscattering from the turbine blades, although it is referred to as forward scattering. The model in the Recommendation assumes perfect conductors for the blades, although they are typically fibreglass or other composite materials, and a scattering pattern based on vertical blade orientation only.

The following analysis assumes that the dimensions of the scattering object are much greater than a wavelength, which then allows a semi-rigorous analysis based on the physical optics approximation. For the low frequency Band III channels, the wavelength is of the order of 2 m. The maximum blade width is about 3 m for typical turbines, but the blades taper to a point, so the assumption that the dimensions are greater than a wavelength is clearly invalid for such low frequencies.

2.2 Analysis of Recommendation ITU-R BT.805 mathematics

Recommendation ITU-R BT.805 is based on the scattering from a rectangular, metallic wind turbine blade in a vertical orientation, as shown in Fig. 1.

FIGURE 1

Geometry of wind turbine blade (rectangular, vertical) and incident and scattered signals

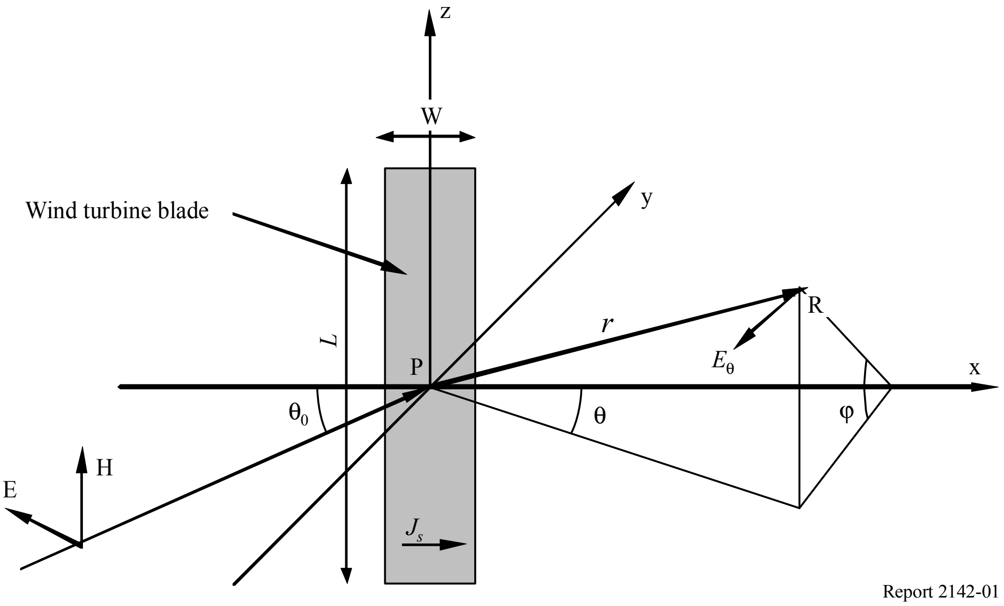

It is assumed the incident signal is horizontally polarized and arrives horizontally at the turbine, as the transmitter is assumed to be a long distance from the wind turbine. The signal scattered from the blade is received at point R with signal strength E_θ at distance r from the blade. Because the blade is assumed to be metallic (infinite conductivity), the surface current density J_s is given by:

$$J_s(x, z) = 2\hat{n} \times H = \frac{2E_0}{\eta} \mathrm{e}^{-jk \cos \theta_0 x} \hat{x} \tag{1}$$

where θ_0 is the incident angle relative to the plane of the blade and E_0 is the incident electric field strength (assumed to be a plane wave). The surface currents re-radiate, resulting in the far field E_θ given by the surface integral:

$$E_\theta = jk\eta \sin\theta \left(\frac{\mathrm{e}^{-jkr}}{4\pi r} \right) \int_{-\frac{W}{2}}^{\frac{W}{2}} \int_{-\frac{L}{2}}^{\frac{L}{2}} J_s(x', z') \, \mathrm{e}^{jk(nx' + mz')} \, \mathrm{d}x' \, \mathrm{d}z' \tag{2}$$

where $k = 2\pi/\lambda$ and $n = \cos\theta$, $m = \sin\theta \sin\varphi$. See Fig. 1 for the definition of the angles.

Upon substituting equation (1) into equation (2) the resulting field at the receiver is given by:

$$\begin{aligned} E_\theta &= \frac{jE_0 \sin\theta}{\lambda} \left(\frac{\mathrm{e}^{-jkr}}{r} \right) \int_{-\frac{W}{2}}^{\frac{W}{2}} \mathrm{e}^{jk(n-n_0)x'} \mathrm{d}x' \int_{-\frac{L}{2}}^{\frac{L}{2}} \mathrm{e}^{jkmz''} \, \mathrm{d}z' \\ &= \frac{j\,AE_0 \sin\theta}{\lambda} \left(\frac{\mathrm{e}^{-jkr}}{r} \right) \mathrm{sinc}\left((n-n_0) \frac{W}{\lambda} \right) \mathrm{sinc}\left(m \frac{L}{\lambda} \right) \end{aligned} \tag{3}$$

where the blade area $A = WL$, $n_0 = \cos\ \theta_0$ and $\mathrm{sinc}(x) = \sin(\pi x)/\pi x$. Therefore the scattering coefficient, ρ, is given by:

$$\rho = \frac{|E_\theta|}{E_0} = \frac{A}{\lambda r}\, g(\theta, \varphi)$$
$$g(\theta,\varphi) = \mathrm{sinc}\left(\frac{W}{\lambda}(\cos\theta - \cos\theta_0)\right)\mathrm{sinc}\left(\frac{L}{\lambda}\sin\theta \sin\varphi\right)\sin\theta \tag{4}$$

In this application, the scattered signal of interest will be close to the horizon, so $\varphi \approx 0$, and the scattering function can be approximated by $g(\theta,\varphi) \approx g(\theta) = \mathrm{sinc}\left(\frac{W}{\lambda}(\cos\theta - \cos\theta_0)\right)\sin\theta$.

For specular reflections $\theta_0 = \theta$, and the scattering function reduces to $g(\theta) = \sin\theta = \sin\theta_0$.

The maximum of the scattering coefficient is given by $\rho_{max} = \frac{A}{\lambda r}$. Recommendation ITU-R BT.805 defines this maximum coefficient at a range of 1 000 m (dB), so that:

$$\Gamma = 20\ \log(\rho_{max}) = 20\ \log(A/\lambda) - 60 \quad \mathrm{dB} \tag{5}$$

However, the scattering spatial function $g(\theta)$ is different from the Recommendation by the incorporation of the additional $\sin\theta$ term, and the additional term associated with the incident angle, which is assumed to be 90° in Recommendation ITU-R BT.805. Note that the Recommendation uses a different definition of angles, namely relative to the normal to the blade, so that the associated Recommendation ITU-R BT.805 expression is:

$$g(\alpha) = \mathrm{sinc}\left(\frac{W}{\lambda}(\sin\alpha - \sin\alpha_0)\right)\cos\alpha \qquad \alpha \approx 0 \tag{6}$$

Therefore Recommendation ITU-R BT.805 applies only when the incident signal is near normal to the blade, whereas equation (4) is valid for all geometries of incident and scattering angles.

2.3 Numerical example

The application of Recommendation ITU-R BT.805 can be illustrated with a numerical example. A wind turbine scatters to a point 1 km from the turbine, as shown in Fig. 2. The wind turbine has three blades, 33 m in length, triangular in shape, and having a base width of 3.3 m. As the model assumes a rectangular blade, it will be assumed that the average width is 1.65 m, so the total area is about 160 m^2. Additional (static) scattering from the tower is ignored in this example.

The wind direction is aligned with the vector between the transmitter and the wind turbine, so the incident signal on the turbine blade is close to normal (the worst case). The frequency is 600 MHz. As the transmitter is assumed to be remote, the direction of the signal at the receiving site and at the wind turbine is assumed to be the same.

FIGURE 2

Geometry for the example. The transmitter is remote, so the drawing is not to scale

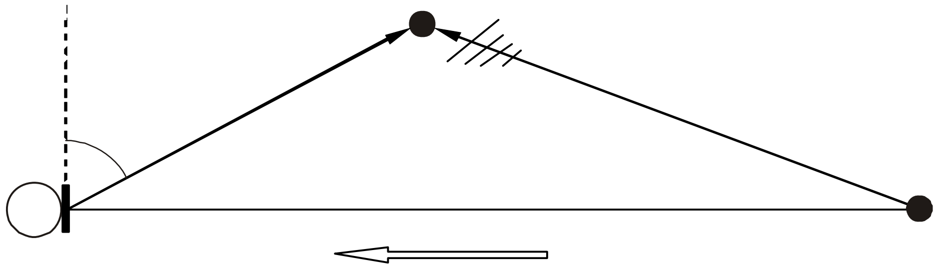

Report 2142-02

The reflection coefficient based on the Recommendation ITU-R BT.805 model is thus:

$$\Gamma = 20\ \log(\rho_{max}) = 20\ \log\left(\frac{A}{\lambda r}\right) = -10 \quad \text{dB} \tag{7}$$

With an omnidirectional antenna, the signal-to-interference ratio (SIR) will therefore be 10 dB. For DTV, the SIR can be equated approximately to the receiver *C*/*N* due to the randomization processing in the receiver, and so the *C*/*N* is well below the typical 20 dB required for DTV planning. It should be noted that this example assumes flat metal blades, which is not typical. Additionally, if a directional antenna were pointed at the DTV transmitter and away from the reflected signal, the directivity of the antenna would be added to the 10 dB; for a typical television antenna with directivity of 12 to 20 dB, this would provide sufficient margin.

It is important to note that the interference signal is due to backscattering, rather than forward scattering as stated in Recommendation ITU-R BT.805. The practical significance is that the directivity of a correctly oriented antenna reduces the observed effects of the scattering from the wind turbine. This is considered in more detail in § 2.4.5.

2.4 Extension of the analysis

This section suggests the issues that should be addressed in modifying Recommendation ITU-R BT.805 model to improve the accuracy of the predictions of the scattered signals. These corrections would apply equally to both analogue and digital television signals.

The issues in the following subsections are components that affect the prediction of the scattered signal. The individual examples are not necessarily related, and the combination of these individual effects is not discussed here. The examples are intended only to illustrate the particular aspects, and are not intended as a comprehensive statement of potential interference from wind farms in general.

2.4.1 Non-metallic turbine blades

Recommendation ITU-R BT.805 assumes metallic (perfectly conducting) wind turbine blades, but actual blades are typically made of fibreglass. As a consequence the Recommendation ITU-R BT.805 model over predicts the level of the scattered signal.

The rigorous calculation of scattering from a non-conducting material can be simplified by an extension of the physical optics principle used in calculating the scattering from a metallic surface. As the surface becomes large relative to the wavelength, the physical optics solution approaches the simple ray optics solution, with the angle of incidence equal to the angle of reflection. For an infinite non-conducting surface with a relative dielectric constant ε_r, the reflection coefficient can be calculated as a function of the angle of incidence. Therefore the scattering from a finite dielectric surface can be obtained by multiplying the solution from a metallic surface by the reflection coefficient calculated for an infinite surface.

The reflection coefficient from a non-conductor depends on the polarization of the signal. For these calculations it is assumed that the polarization is horizontal. The reflection coefficient for horizontal polarization is given by:

$$\rho_E = \frac{\varepsilon_r \cos\theta - \sqrt{\varepsilon_r - \sin^2\theta}}{\varepsilon_r \cos\theta + \sqrt{\varepsilon_r - \sin^2\theta}} \tag{8}$$

where θ is the incident angle relative to the normal to the surface, and ε_r is the relative dielectric constant and is greater than 1. For fibreglass typically used in wind turbine blades the relative dielectric constant is about 4. The main practical interest when the incident angle is near the normal (θ is small), so that equation (8) becomes:

$$\rho_E \approx \frac{\varepsilon_r - \sqrt{\varepsilon_r}}{\varepsilon_r + \sqrt{\varepsilon_r}} \tag{9}$$

For $\varepsilon_r = 4$, this gives a reflection coefficient of 1/3, or –10 dB. The reflection coefficient is not very sensitive to the exact value of the dielectric; for a value of $\varepsilon_r = 9$, which results in $\rho_E = 1/2$ or –6 dB. Thus the inclusion of this electric field reflection coefficient is important in assessing the overall scattered signal from wind turbines. In particular, based on the above analysis, Recommendation ITU-R BT.805 overestimates the scattered signal by about 6 to 10 dB.

2.4.2 Triangular turbine blades

Recommendation ITU-R BT.805 assumes that the wind turbine blades are rectangular, while actual turbine blades are close to triangular. Therefore the calculations need to use a triangular shape for the surface integral in equation (3). The only modification is that the limits in the x-coordinate are replaced by:

$$w(z) = \frac{W}{2}\left(1 - \frac{z}{L}\right) \tag{10}$$

so that surface integral becomes:

$$E_\theta = \frac{jE_0 \sin\theta}{\lambda}\left(\frac{\mathrm{e}^{-jkr}}{r}\right)\int_{-w(z)}^{w(z)}\int_{-\frac{L}{2}}^{\frac{L}{2}} \mathrm{e}^{jk(n-n_0)x'}\mathrm{e}^{jkmz''}\,\mathrm{d}x'\mathrm{d}z' \tag{11}$$

Again the assumption is made that the signal is measured near the horizon, so that $m = 0$ in equation (11). With this simplification the integral can be evaluated to give:

$$E_\theta = \frac{j\,\Delta E_0 \sin\theta}{\lambda}\left(\frac{\mathrm{e}^{-jkr}}{r}\right)\mathrm{sinc}^2\left((n-n_0)\frac{W/2}{\lambda}\right) \tag{12}$$

where $\Delta = LW/2$ is the area of the triangular blade. The scattering coefficient ρ is therefore:

$$\rho = \frac{|E_\theta|}{E_0} = \frac{A}{\lambda r}\, g(\theta)$$
$$g(\theta) = \mathrm{sinc}^2\left(\frac{\overline{W}}{\lambda}(\cos\theta - \cos\theta_0)\right)\sin\theta \tag{13}$$

where A is the area of the blade, and $\overline{W}$ is the mean width of the blade. The form of this expression is the same as for the rectangular blade (with the appropriate definitions of the area and the mean width), but with a different scattering pattern $g(\theta)$.

Because on average the triangular blade is narrower than a rectangular blade with the same width at the base, the scattering pattern will be broader. The relative scattering coefficient as a function of θ is illustrated in Fig. 3. It is clear that the scattering pattern for the triangular blade is broader and has smaller side-lobes. Note also that Recommendation ITU-R BT.805 suggests that scattering away from the main direction has a magnitude of about –10 dB (or 0.32 on the scale in the figure below). It is not clear how this value was derived.

FIGURE 3

Relative scattering patterns (as a ratio) for rectangular and triangular blades.
The blade base width is 2.35 m with the incident signal normal to the blade.
Frequency = 600 MHz

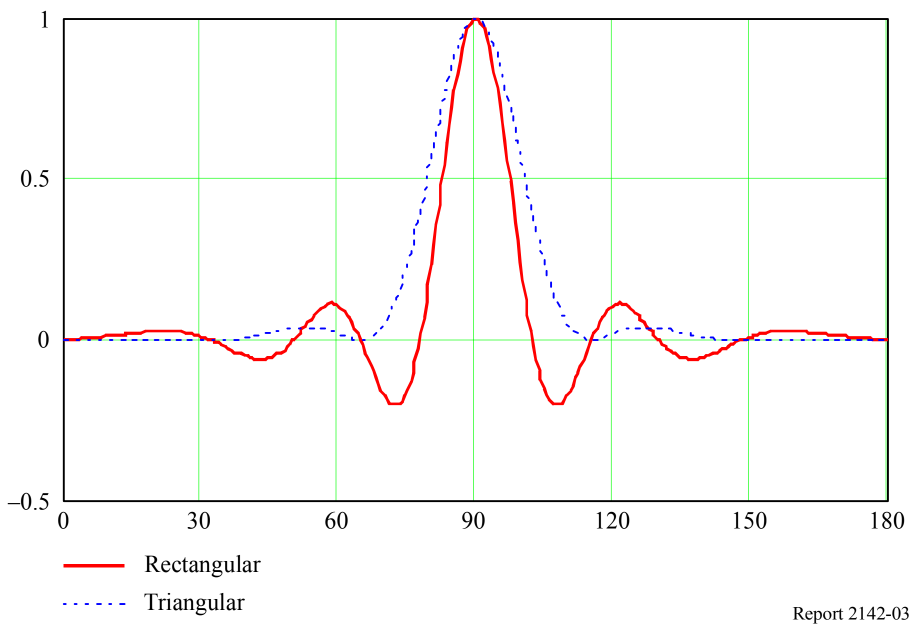

Figure 4 shows the polar pattern of scattering from the turbine blades (as pictured in Fig. 5). The scattering is largely confined to the backscattering and forward scattering directions, with the backscattering about 13 dB greater than the forward scattering. This result is similar to that obtained for the turbine pylon described below. In contrast, Recommendation ITU-R BT.805 states that the dominant scattering is in the forward scattering direction.

FIGURE 4

Polar pattern of the scattering (dB) from the turbine blades, showing the backscattering (right) and the forward scattering (left). The backscattering level is about 13 dB greater than forward-scattering. One blade is vertical, so scattering is symmetric about the horizontal axis

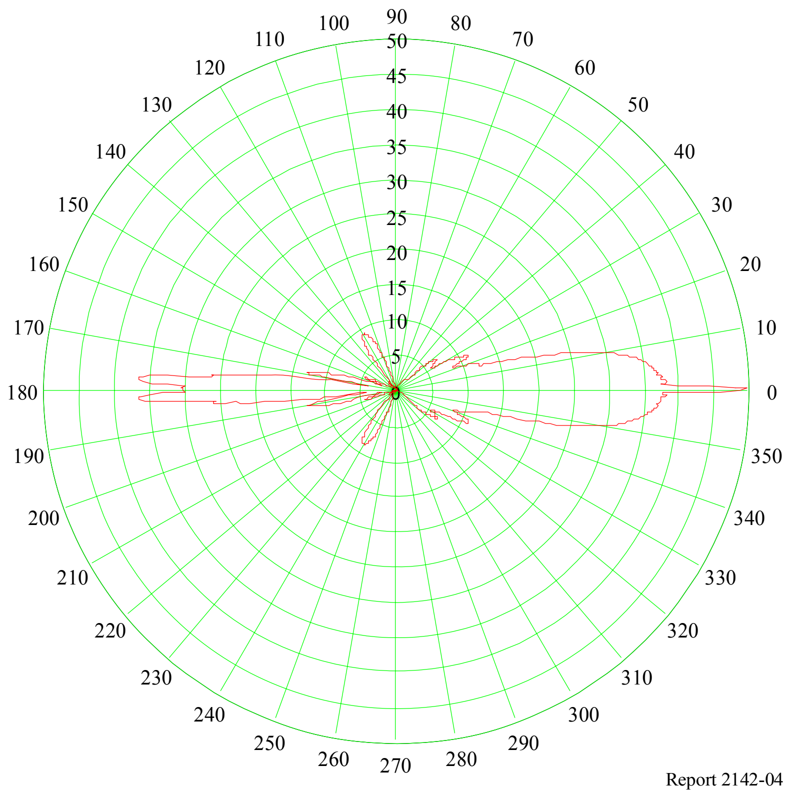

Report 2142-04

FIGURE 5

Geometry of wind turbine surfaces. Total rotor area is 160 m^2.
Diagram not to scale

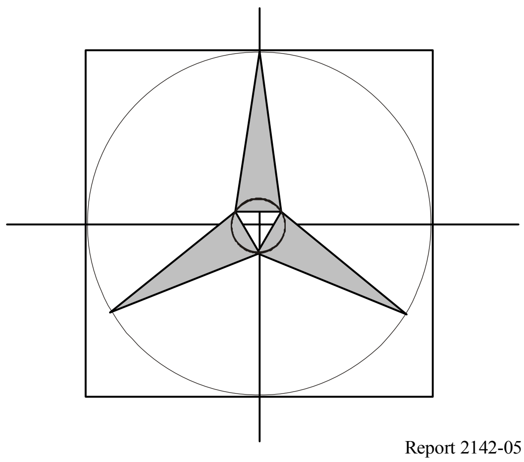

Report 2142-05

2.4.3 Arbitrary orientation of turbine blades

The calculations in the previous sections were based on the assumption that the wind turbine blade is vertical. However, with rotating blades the orientation is constantly changing and this must be taken into account.

The analysis of the scattering from a blade at an arbitrary orientation is similar to the vertical case with an adjustment to the surface integral. For the far-field case, the surface integral can be interpreted as a two-dimensional Fourier transform. However, at 600 MHz with a 30 m blade (diameter 45 m for three blades) the far-field range, given by $R = 2D^2/\lambda$, is 8 km. Therefore a near-field analysis is required. This is done by approximating the phase variation by a second-order function using Fresnel zone analysis. Although the following computations are complicated, they are much faster to implement than a numerical method for the same situation.

Using the geometry in Fig. 6, the receiver at range r from the coordinate reference point is at:

$$P(x, y, z) = r(\cos\theta, -\sin\theta\cos\varphi, \sin\theta\sin\varphi) \tag{14}$$

Thus the range R to a point $Q(x, z)$ on the blade (in the x-z plane) is given by:

$$\begin{aligned} R &= \sqrt{(r\cos\theta - x)^2 + (r\sin\theta\cos\varphi)^2 + (r\sin\theta\sin\varphi - z)^2} \\ &= \sqrt{r^2 + x^2 + z^2 - 2rx\cos\theta - 2rz\sin\theta\sin\varphi} \end{aligned} \tag{15}$$

FIGURE 6

Geometry of the propagation path from a point (x, z) on the blade to the receiver

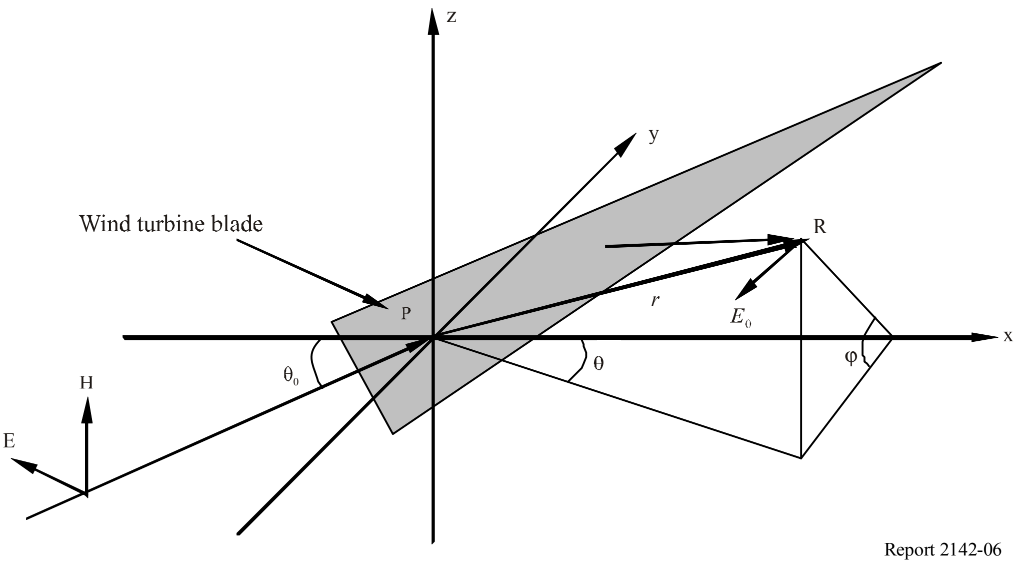

The Fresnel (second order) approximation to the range R is:

$$R(x, z) \approx r - x\cos\theta - z\sin\theta\sin\varphi + \frac{x^2}{2r}\sin^2\theta + \frac{z^2}{2r}\left(1 - \sin^2\theta\sin^2\varphi\right) \tag{16}$$

To evaluate the surface integral over the triangular blade for an arbitrary rotation (ψ) of the blade, a new coordinate system (u, y, v) is used to conserve the symmetry of the blade:

$$\begin{aligned} x &= u\cos\psi - v\sin\psi \\ z &= u\sin\psi + v\cos\psi \end{aligned} \tag{17}$$

Equation (16) can then be approximated as:

$$\begin{aligned} R(u,v) \approx{}& r - (\cos\theta\cos\psi + \sin\theta\sin\varphi\sin\psi)u - (\sin\theta\sin\varphi\cos\psi - \cos\theta\sin\psi)\,v + \\ & \frac{u^2}{2r}\left[1-(\cos\psi\cos\theta+\sin\theta\sin\varphi\sin\psi)^2\right] + \frac{v^2}{2r}\left[1-(\sin\theta\sin\varphi\cos\psi-\cos\theta\sin\psi)^2\right] \end{aligned} \tag{18}$$

A similar expression can be derived for the incident path ($R_0(u, v)$) from the transmitter, but as the transmitter is in the far field, only the first order (linear) terms in (u, v) need to be included to give the required accuracy. The phase from transmitter to blade to the receiver can be expressed as:

$$\Phi(u,v) = \exp[-jk(R_0(u,v) + R(u,v)))] \tag{19}$$

By substituting, the signal phase is given approximately by:

$$\begin{aligned} &\Phi(u,v) \approx \exp[-jk(r_0+r)]\exp\left[j(\alpha u + \beta v - \gamma u^2)\right] \\ &\alpha = k[(\cos\theta - \cos\theta_0)\cos\psi - (\sin\theta\sin\varphi - \sin\theta_0\sin\varphi_0)\sin\psi] \\ &\beta = k[(\sin\theta\sin\varphi - \sin\theta_0\sin\varphi_0) + (\cos\theta - \cos\theta_0\sin\psi)] \\ &\gamma = \frac{k}{2r}\left[1-(\cos\theta\cos\psi+\sin\theta\sin\varphi\sin\psi)^2\right] \end{aligned} \tag{20}$$

With these approximations to the phase, and assuming that for the calculation of amplitude, the range from points on the blade to the receiver are the same, the scattered field can be evaluated as:

$$\begin{aligned} &E_\theta = \frac{jE_0\sin\theta}{\lambda}\left(\frac{e^{-jkr}}{r}\right)\left\{\int_{L_0}^{L+L_0} e^{j(\alpha u - \gamma u^2)}\left[\int_{-w(u)}^{w(u)} e^{j\beta v}\mathrm{d}v\right]\mathrm{d}u\right\} \\ &w(u) = \frac{W}{2}\left(1-\frac{u-L_0}{L}\right) \end{aligned} \tag{21}$$

where W is the width of the blade at its base, L is the length of the blade, and L_0 is the distance from the axis of the rotor to the base of the blade.

This can ultimately be solved to give the following expression:

$$E_\theta = \frac{jE_0\sin\theta}{\lambda}\left(\frac{e^{-jkr}}{r}\right)\{\, I(a,b,c,1) - I(a,b,c,0)\} \tag{22}$$

where:

$$a = \frac{\beta W}{2} \qquad b = L\left(\alpha - 2\gamma\left(L_0 + L\right)\right) \qquad c = \gamma L^2 \tag{23}$$

and $I(a,b,c,x)$ is given by the following equations, depending on β.

For $\beta \neq 0$:

$$\begin{aligned}
I(a,b,c,x) &= \frac{1}{4\sqrt{c}}\left[M\sqrt{\pi}\exp\left(j\frac{(a-b)^2}{4c}\right)\left\{f(-a,b,c,x) - \exp\left(j\frac{ab}{c}\right)f(a,b,c,x)\right\}\right] \\
f(a,b,c,x) &= \mathrm{erf}i\left[\frac{M}{2\sqrt{c}}\left(a+b+2cx\right)\right] \\
\mathrm{erf}i(z) &= -j\,\mathrm{erf}(jz) \qquad M = \frac{j-1}{\sqrt{2}}
\end{aligned} \tag{24}$$

and for $\beta \rightarrow 0$:

$$\begin{aligned}
I(a,b,c,x) &= \frac{1}{2c}\left[\frac{b}{2}\sqrt{\frac{j\pi}{c}}\exp\left(j\frac{b^2}{4c}\right)f(b,c,x) + j\exp\left(-jx\left(b+cx\right)\right)\right] \\
f(a,b,c,x) &= \mathrm{erf}i\left(M\left(\frac{b+2cx}{2\sqrt{c}}\right)\right)
\end{aligned} \tag{25}$$

This solution is demonstrated for three cases, using the near-field formula derived above, a far-field solution, and a numerical approximation with a pixel size of 1/8 of a wavelength. Note that, for simplicity, these examples use perfectly conducting blades, and that in real analysis, the effect of the non-metallic structure would have to be included.

Figure 7 shows the scattering from a three-blade rotor with one blade vertical, giving a symmetric horizontal pattern. As the rotor consists of vertically and horizontally large dimensions the scattering pattern has both broad and narrow components. The far-field solution overestimates the scattering coefficient, and there is good agreement between the numerical and near-field solutions.

Figure 8 shows the scattering with the rotor rotated 90º anti-clockwise, giving an asymmetric scattering pattern. The scattering pattern is similar to the previous case, but the main beam is wider and the broad beam less prominent. These two examples illustrate the changing scattering pattern as the wind turbine rotates.

Figure 9 shows the scattering coefficient from a three-blade rotor as the blades rotate through 360º. The far-field and near-field solutions have broadly similar characteristics, but the far-field solution is shifter slightly by about 10º relative to the near-field (true) position. The scattering pattern has six peaks within the 360º; as the three blades and mirror image patterns result in similar scattering. However, overall the pattern repeats three times as expected for a three-blade rotor.

FIGURE 7

Scattering coefficient from three-blade rotor with one blade vertical. Range 1 km, pylon height 67 m, receiver height 67 m. Incident signal normal to blade

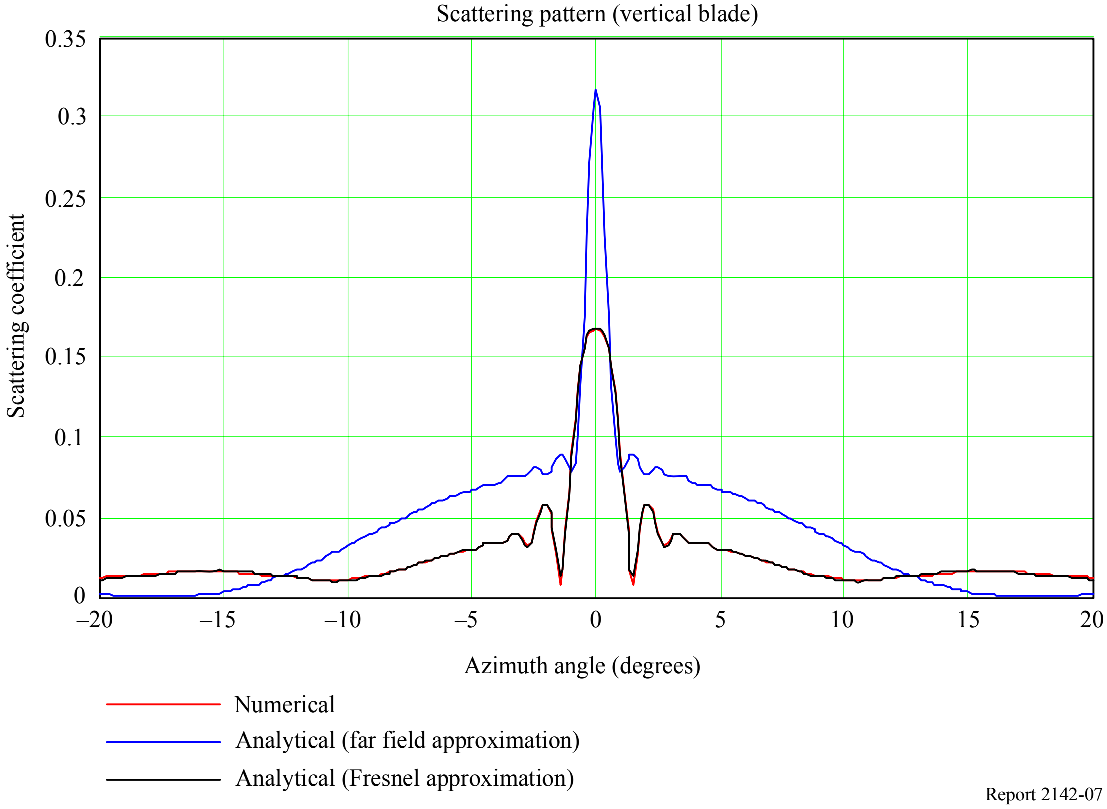

FIGURE 8

As in Fig. 7 but with one blade horizontal. The far-field solution is (erroneously) symmetric, but the numerical and Fresnel solutions are asymmetric

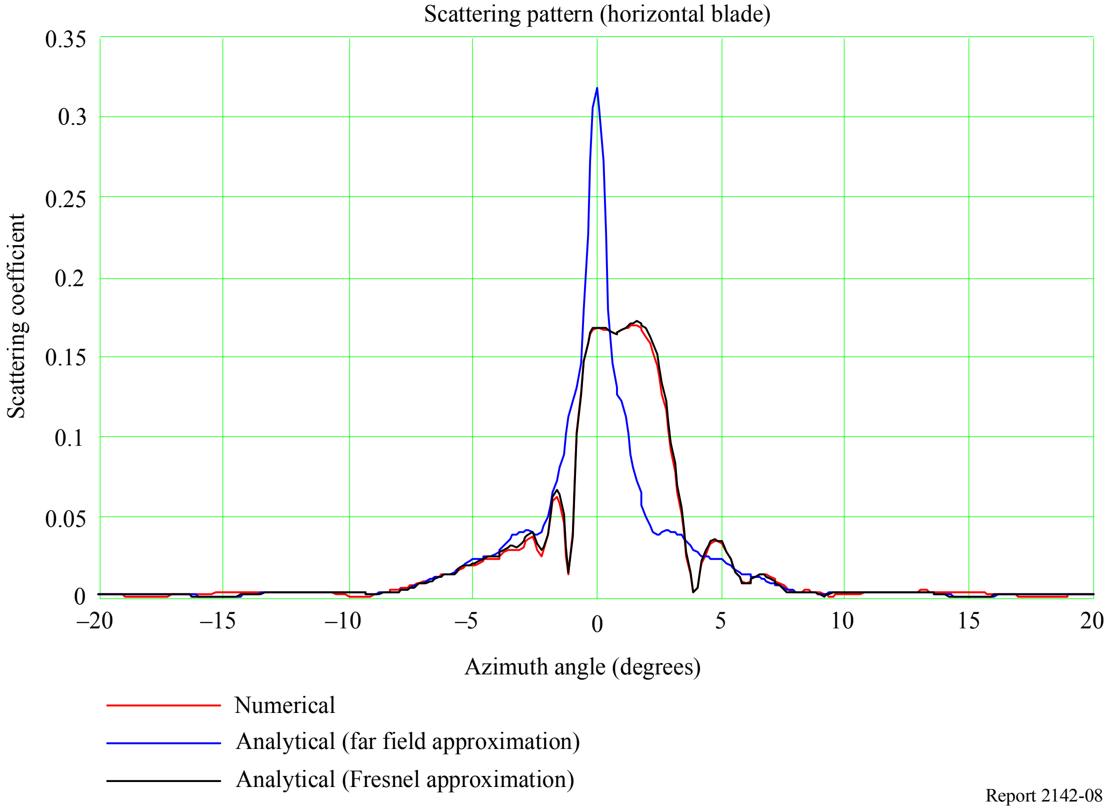

FIGURE 9

Scattering coefficient from a three blade rotor. Pylon height 67 m. Incident signal normal to blade. Receiver is 1 km from the blade, 10 m above ground, and at an azimuth angle of 85° relative to the plane of the blade. The far field solution is shifted by about 10° relative to the Fresnel zone (true) position

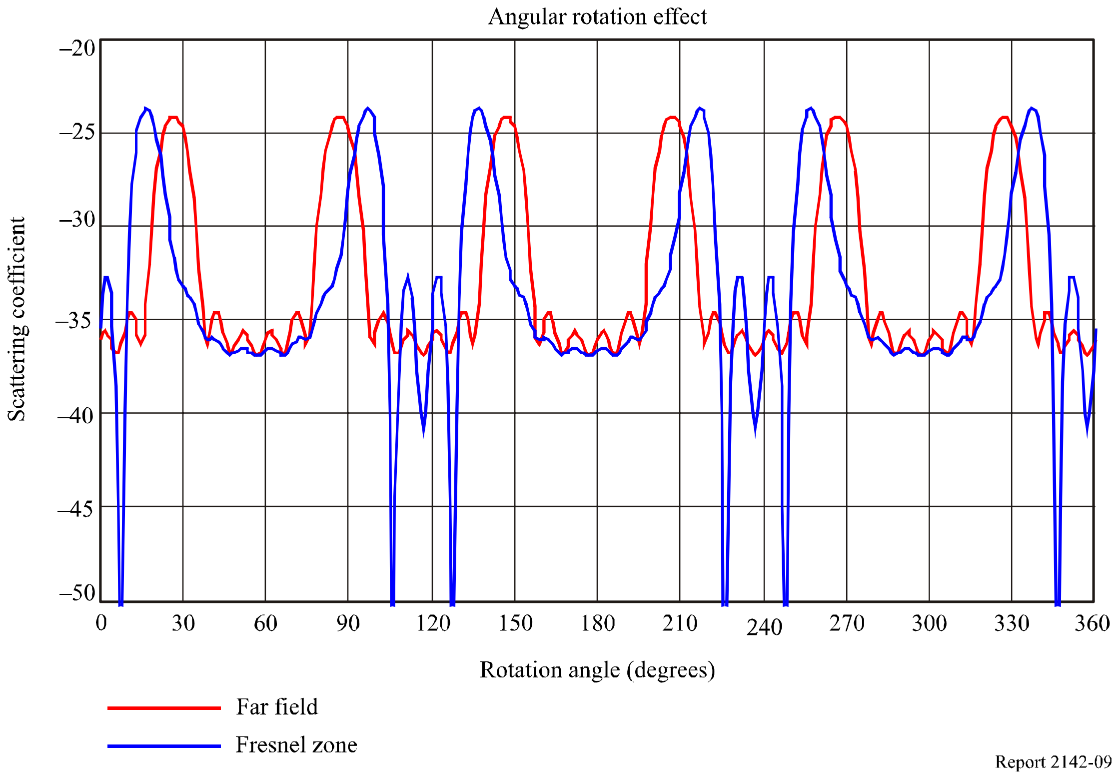

The main conclusion is that at positions of practical interest, the scattering pattern will vary by at least 10 dB, with (for a three-bladed turbine) a dominant frequency component of six times the rotation rate or about 3 Hz for a typical rotation rate of 20 rpm.

2.4.4 Scattering from pylon

As the support pylon of the wind turbine is a large metallic structure, the scattering from the pylon must also be considered. Wind turbine pylons are typically tapered (typically 0.5° to 1°) cylindrical structures, and scattering calculations can be based on a conducting cylinder with a diameter equal to the mean of the actual pylon. The pylons used in the following example have a base diameter of 4.2 m and a top diameter of 2.3 m, giving a mean diameter of 3.25 m. The height is 68 m and the taper is 0.8°.

The rigorous expression for the scattering coefficient from an infinite conducting cylinder for a vertically polarized plane wave is given by:

$$\Gamma_v = \frac{E_s}{E_0} = \sum_{n=0}^{\infty} \varepsilon_n (-j)^n J_n(ka) \frac{H_n^{(2)}(kr)}{H_n^{(2)}(ka)} \cos(n\varphi) \tag{26}$$

where ε_n is the Neumann's number ($\varepsilon_n = 1$ when $n = 0$ and $\varepsilon_n = 2$ when $n \neq 0$), a is the radius of the cylinder, and φ is the horizontal scattering angle relative to the incident propagation direction.

The corresponding expression for horizontal polarization is given by:

$$\Gamma_h = \frac{E_s}{E_0} = -j \sum_{n=0}^{\infty} \varepsilon_n (-j)^n J'_n(ka) \frac{H_n^{(2)}(kr)}{H_n'^{(2)}(ka)} \cos(n\varphi) \tag{27}$$

where the "dash" on the Bessel and Hankel functions represents the derivative of the function. While these two expressions are different, as the diameter of the cylinder becomes large relative to wavelength, the two expressions approach the same solution. For example, in Fig. 10 the diameter is 6.6 wavelengths, and the shape of the two curves is very similar.

The computed scattering coefficient from an infinite cylinder with a diameter of 3.3 m is shown in Fig. 10. The scattering pattern consists of a strong backscatter (scattering coefficient 0.158 or –16 dB for vertical polarization, 0.139 or –17 dB for horizontal polarization), and an approximately constant value in the range to 0.02 to 0.03 (–34 dB to –30 dB) at angles greater than 10° from the peak reflection. Thus the scattering in the horizontal plane is confined to a narrow 3 dB beamwidth of ±3.5°.

FIGURE 10

Computed scattering coefficient in the horizontal plane from an infinite cylinder, diameter 3.3 m, range 1 km.
Frequency = 600 MHz

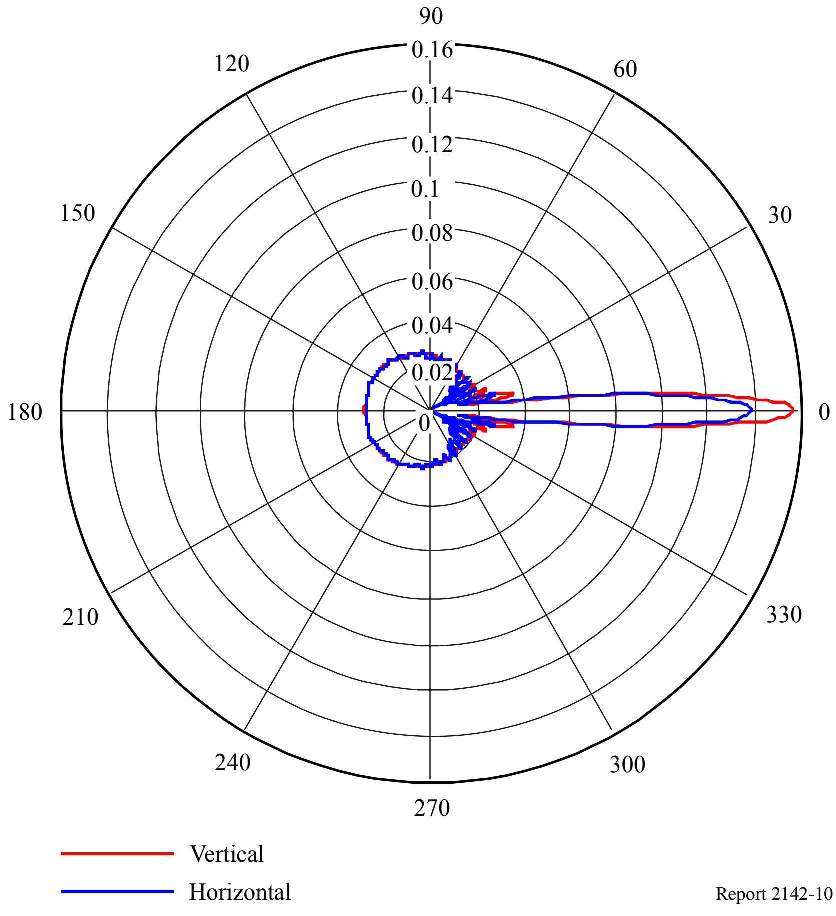

The behaviour of the reflection coefficient as a function of range is shown in Fig. 11. As the radiation at a long range from an infinite cylinder approaches that of a pure cylindrical wave, the amplitude of the scattered signal varies as $1/\sqrt{r}$ at long range (or a 3 dB reduction for each doubling of range). In practice the scattered signal can be considered cylindrical only relatively close to the pylon, so the effect of the finite height must be considered for any practical predictions at long range. The following analysis estimates the correction factor to adjust the infinite cylinder solution to the finite length case, and provides an estimate of the vertical scattering beam pattern.

FIGURE 11

Computed scattering coefficient from an infinite cylinder as a function of range

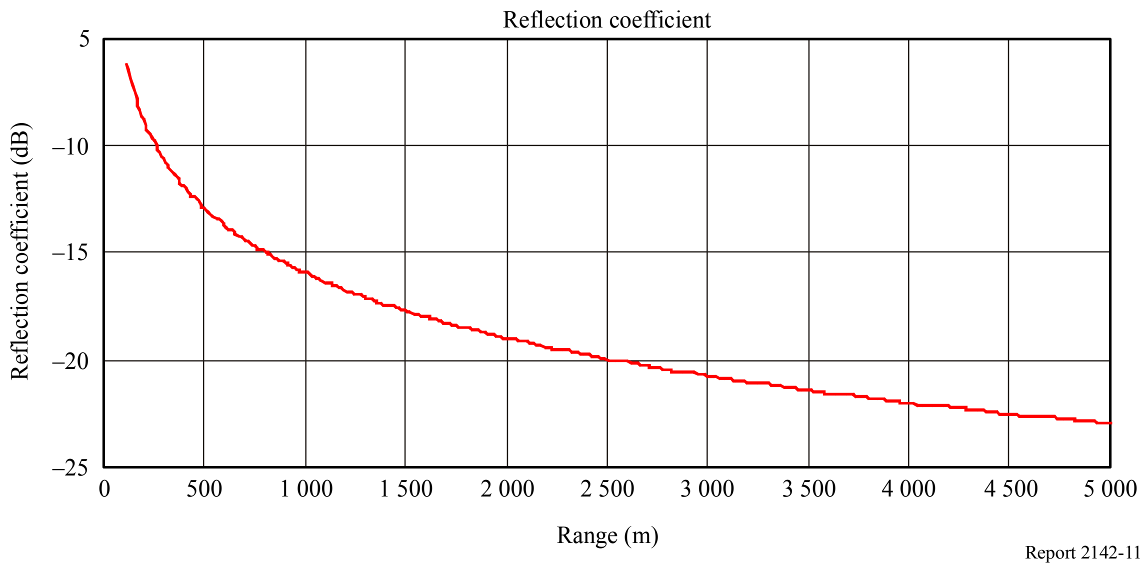

The correction factor for the finite case is estimated using a numerical physical optics solution. It is assumed that the incident signal is horizontal, and the vertical scattering angle relative to the horizon is θ, as shown in Fig. 12.

FIGURE 12

Geometry of the scattering from a finite height cylinder

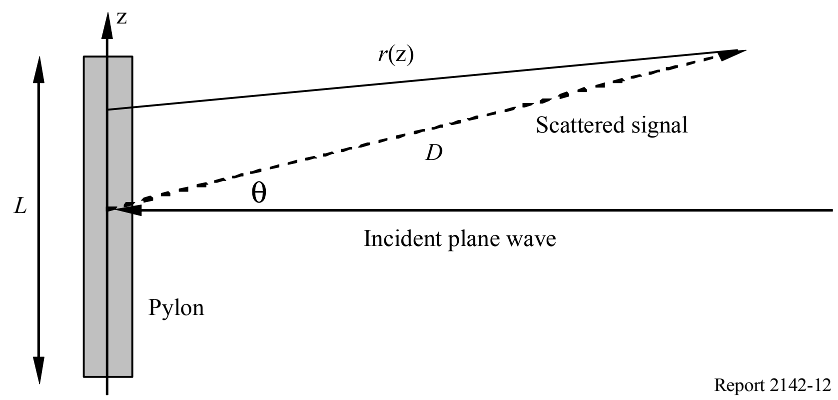

The effect of the pylon height and range is based on the vertical integral:

$$I_{vert} = \int_{-\frac{L}{2}}^{\frac{L}{2}} e^{-jkr(z)} \, dz \approx 2e^{-jkD} \int_{0}^{\frac{L}{2}} e^{-j\frac{kz^2}{2D}} \, dz \tag{28}$$

where D is the horizontal range from the pylon, and L is the height of the pylon. The integral can be evaluated to give:

$$I_{vert}(\theta, D, L) = \frac{\sqrt{\lambda D}}{\sqrt{2}\cos\theta} e^{j(\alpha - kD)} \left[CS\left(\eta\left[\frac{L}{2}\right]\right) - CS\left(\eta\left[-\frac{L}{2}\right]\right)\right]$$

$$\alpha = \pi \frac{r}{\lambda} \tan^2 \theta \tag{29}$$

$$\eta(z) = \sqrt{\frac{2D}{\lambda}} \left(\frac{z}{D} \cos\theta - \tan\theta \right)$$

$$CS(x) = C(x) - jS(x)$$

where $C(x)$ and $S(x)$ are the cosine and sine Fresnel integrals. The complex Fresnel integral $CS(x)$ can be expressed in terms of the error function by:

$$CS(x) = \frac{1-j}{2} \operatorname{erf}\left(\frac{\sqrt{\pi}}{2} [1+j] x \right) \tag{30}$$

As the height of the pylon becomes large the integral approaches the limiting solution:

$$I_{vert}(\theta, D, \infty) I = \left(\frac{\sqrt{\lambda D}}{\cos\theta} \right) e^{j(\alpha - kD - \pi/4)} \tag{31}$$

which shows that the effective height of the pylon in terms of scattering is of the order of $\sqrt{\lambda D}$. For example, at a range of 1 km and a frequency of 600 MHz, the effective height is about 22 m. As the actual height is 68 m, in this case the infinite approximation is satisfactory.

For a scattering angle of $\theta = 0$ the normalization factor N is the ratio of the finite length cylinder solution to the infinite cylinder solution:

$$N(D) = \frac{I_{vert}(0, D, L)}{I_{vert}(0, D, \infty)} = \sqrt{2} e^{j\pi/4} CS\left(\frac{L}{\sqrt{2\lambda D}} \right) \tag{32}$$

The scattered signal correction factor for a 68 m pylon is shown in Fig. 13 for ranges up to 5 km. The correction factor is ±2 dB up to a range of 5 km for a frequency of 600 MHz, but at lower frequencies the correction factor is larger. Therefore at long range (particularly at lower frequencies) the scattered signal is somewhat smaller than that predicted by the infinite cylinder model, but the correction factor does not exceed ±2 dB for ranges up to 1.5 km. From equation (32) the correction factor can be ignored provided the argument of the Fresnel integral functions is large. In practice, a suitable constraint is:

$$\frac{L}{\sqrt{2\lambda D}} > 1 \qquad \text{or} \qquad D < \frac{L^2}{2\lambda} \tag{33}$$

For a pylon height of 68 m the maximum ranges are 1 150 m, 2.3 km and 4.6 km at frequencies of 150 MHz, 300 MHz and 600 MHz respectively.

FIGURE 13

Scattered signal correction factor for a 68 m high pylon (at three frequencies) as a function of range from the wind turbine. This value modifies the scattering coefficient from an infinite cylinder as given in Figs. 10 and 11

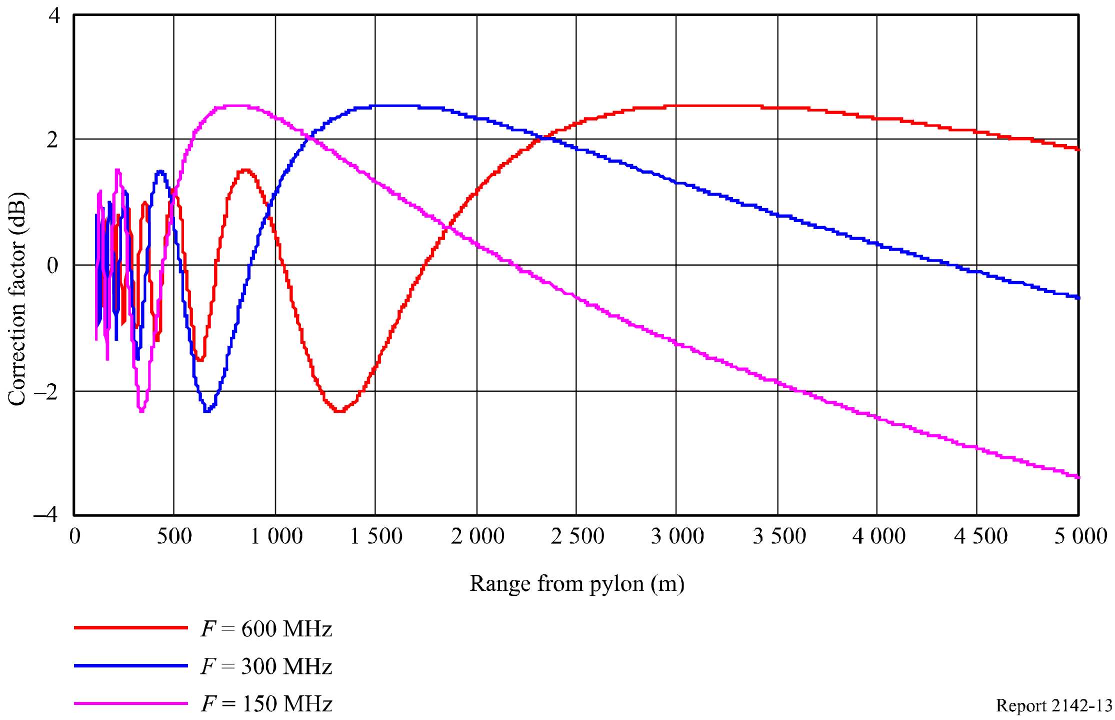

The vertical scattering pattern can also be computed from equation (29). Figure 14 shows three examples at ranges of 250, 500 and 1 000 m. It is clear that the beamwidth decreases as the range increases. From equation (29) it can be shown that the beamwidth is of the order of:

$$BW \approx \pm\frac{L}{2D} \qquad \text{rad} \tag{34}$$

For the above three ranges the corresponding beamwidths are ±8°, ±4° and ±2° which agrees generally with Fig. 14.

At close range the scattering amplitude is approximately constant within a band of elevation angles, and the scattering in this band can be approximated by an infinite cylinder. As the range increases the beamwidth decreases, but an asymptotic limit is reached at a longer range.

FIGURE 14

Computed scattering pattern in the vertical plane different ranges from a pylon of height 68 m and a frequency of 600 MHz

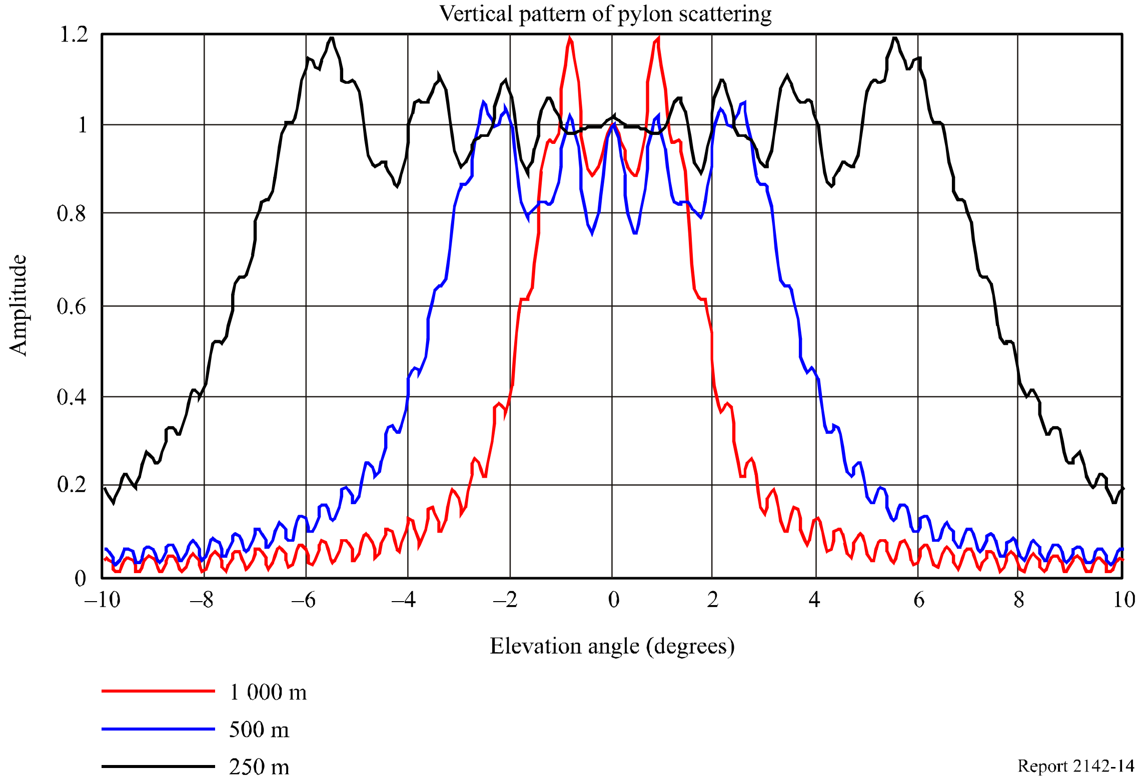

2.4.5 Effect of antenna directivity and reception geometry

It is assumed that in suburban and rural areas an antenna with reasonable directivity (12-20 dB) is used for television reception. The relative level of the direct and scattered signals will be influenced strongly by the antenna directivity in the direction of the direct and scattered signals. Three cases may be considered.

In the first case, shown in Fig. 14, the signals are scattered from the turbine and arrive at the television antenna from the back. In this case the scattered signal is at its maximum, but will be significantly moderated by the antenna front-to-back ratio. Using (as an example only), a scattering coefficient of –15 dB, the signal-to-interference ratio will be at 27 to 35 dB, above the interference threshold of 20 dB used in digital TV planning.

In the second case, shown in Fig. 15, the antenna directivity is similar for both the direct and scattered signals. However, the forward scattered signals are considerably smaller, even if the turbine is in direct line of sight. This geometry therefore combines lower scattered signal with no mitigating effect from the antenna directivity. In this case, the interference performance is approximately similar to the first case.

In the third case, which is more typical of rural Australian wind farms, the turbines are located on the top of a ridge, in the direct line of the television signals. The television receiver is in a valley without line-of-sight (LoS) to the television transmitter. In such circumstances the incident television signal at the wind turbines will be much greater than the wanted signal at the television receiving antenna. Because of the potentially wide range of conditions, no particular numerical case is given, but an incident signal difference of 20-30 dB is not unreasonable. A particularly difficult case is the geometry shown in Fig. 16. The directivity of the television receiver antenna does not provide any protection from the interference scattered from the turbine.

FIGURE 15

Geometry of minimal scattering and no protection from the antenna directivity

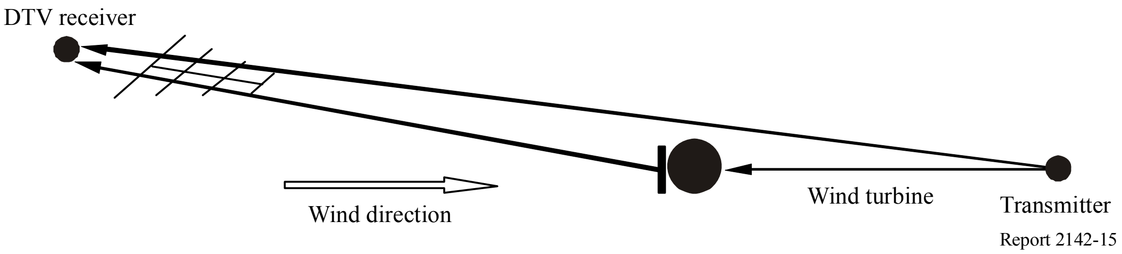

FIGURE 16

Geometry which could result in a large interference signal relative to the “direct” signal

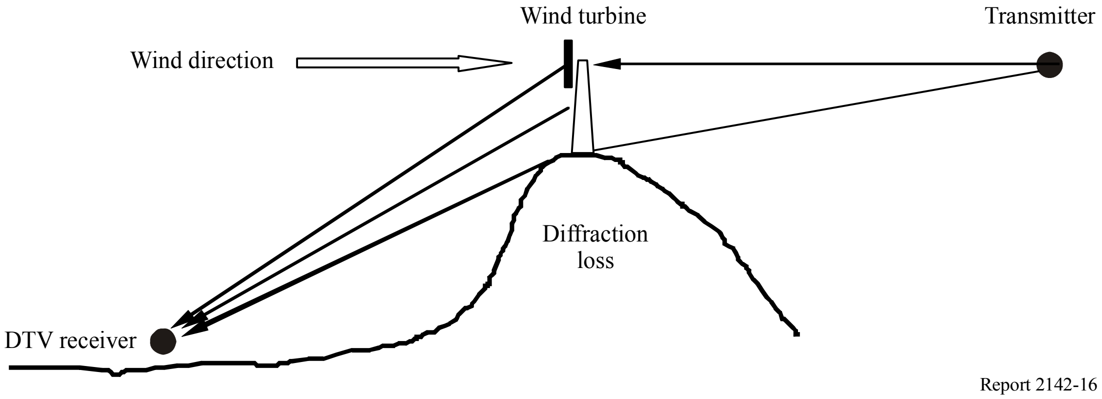

The overall conclusion is that the geometry and local terrain are critical in determining the interference effects from wind turbines.

Annex 2

1 Introduction

The study in Annex 1 is a study based on theoretical modelling that identified Recommendation ITU-R BT.805 is not adequate for predicting interference from wind farms for analogue and digital TV signals.

The study described in this annex indicates that the methods to assist in quality assessment of the coverage and service area for digital television broadcasting in System B in Recommendation ITU-R BT.1735 are not satisfactory for the type of dynamic signal variations from rotating wind turbine blades.

1.1 Overview of study

This text is part of a study to determine the effect on digital television reception due to interference arising from scattering from multiple wind turbines (referred to as a wind farm). Annex 1 provided theoretical and computer simulation studies of the scattering of radio signals from the wind turbine structure, both from the static pylon and the dynamics from rotating blades. In this Report, the work is extended to measurements of the interference effects from multiple wind turbines, as well as computer simulations to predict performance of digital television receivers using information about the size and shape of wind turbines and the geographical layout of a wind farm.

Measurements reported in this text were made around the Challicum Hills wind farm, near Ararat in Victoria, Australia. Figure 17 shows a surface map of the test area, with the wind farm at the lower left, and the transmitter on Lookout Hill at the upper right. The measurements, performed by the Commonwealth Scientific and Industrial Research Organisation (CSIRO), logged actual TV signals as files of digital data that can be analysed for multipath interference using a software receiver program. The logged signals also provide a reference signal with little multipath corruption, which can be used to generate simulated television signals with specific multipath interference. The multipath scattering impulse response can be estimated from the measurements. This provides the scattering coefficient, a single statistical parameter which represents the scattered signal relative to the incident signal and therefore summarizes the overall level of multipath interference at a point.

The measured or simulated television signal is processed by a software receiver, which performs the same signal processing as in an actual receiver, although limited to decoding the pilot signals to calculate the propagation impulse response. The software also estimates the channel bit error rate[1] (CBER) and the modulation error ratio MER, which can be used to specify the "quality" of the received signal. Although the measurement data come from specific multipath interference cases, the relationship between the CBER or MER and the scattering coefficient provides a generally applicable result.

The wind farm is located on rolling hills 100-150 m above the surrounding largely flat grazing land. There is direct LoS from the transmitter to the wind turbine on the hills. The main interference area is expected in the shadow of the hills at the lower left.

In addition to the measurements, software has been developed to estimate the EM scattering as a function of the size and shape of the wind turbines, the geometry of the wind farm, the location of the transmitter, and the receiving location. This was initially reported in Document 6E/398 but has been extended to arbitrary wind farm geometries. Maps of the scattering coefficient, MER and CBER can be calculated as a function of receiving position, which are useful in identifying areas where significant interference can be expected. The multipath impulse response can also be calculated, which when combined with the measured reference signal produces an artificial television signal for the location of interest. This can then be fed into the software receiver to estimate the CBER and MER.

The calculation of scattered signals from wind turbines and wind farms, as well as more general charts of digital television receiver performance as a function of the scattering coefficient, could be useful in the ongoing development of Recommendation ITU-R BT.805.

[1] The channel BER is the raw bit error rate before the Viterbi error correcting.

FIGURE 17

Surface map of the measurement area

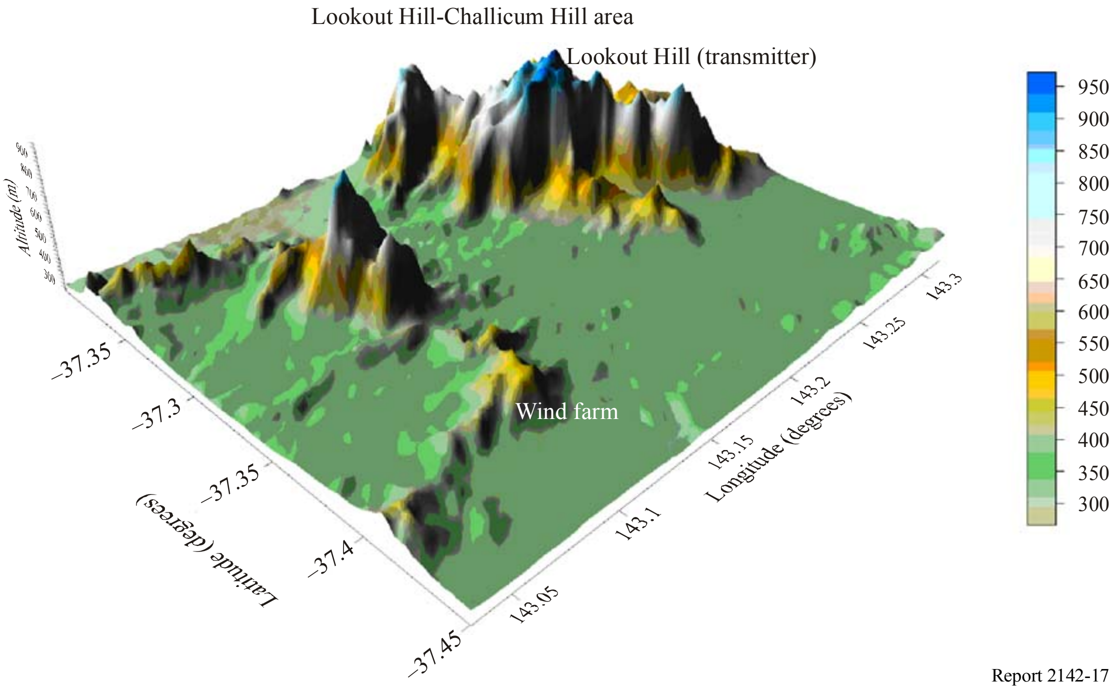

Report 2142-17

1.2 Measurement overview

The measurement programme was a joint effort between the CSIRO ICT Centre and Free TV Australia[2], over a period of three days (2-4 May 2006). The CSIRO measurements used a custom receiver and data logger to record the receiver IF analogue output in order to capture and analyse the fast-varying signals associated with the rotation of wind turbine blades. The Free TV Australia measurements were made using a 4T2 commercial test instrument, which logs a wide range of *average* signal parameters. This report concentrates on the analysis of the CSIRO data.

The measurements were made at eight locations surrounding the wind farm. The extent of scattering from wind turbine blades depends on the direction of the wind relative to the transmitter and receiver location(s). Unfortunately, the weather conditions on the first two days produced minimal blade scattering. On the third day the wind direction was more favourable, but still not optimum, for interference from the blades. Data from the third day shows the dynamic effects of interference from wind turbines on the reception of digital television signals.

2 Predicted performance with software models

2.1 Overview

Predictions for the scattering from a specific wind farm were based on the calculation of scattering from wind turbines as described in Annex 1, and on software to implement the front-end signal processing of a digital television receiver. In the second case, the input signal was synthesized from received signals recorded at the CSIRO Radio Physics Laboratory at Marsfield in Sydney, Australia using a roof-mounted high-gain antenna to provide a good reference with minimal multipath.

[2] Free TV Australia is an industry body which represents all of Australia's commercial free-to-air television licensees.

This was then used as input to the simulation program to generate a synthesized multipath signal at specific locations near the wind farm. The synthesized signal is an input to the software receiver to estimate the channel bit error rate and the modulation error ratio.

2.2 Geographic summary

Figure 18 shows the layout of the wind farm, with 35 turbines in an area of about 5 km^2, in three approximately linear groups along ridge lines. The altitude (at the base of the pylons) is between about 430 and 510 m. The surrounding land is approximately flat with a mean altitude of about 350 m. As the pylons are 68 m tall, the axis of the turbine rotors is about 150-200 m above the surrounding land where the interference effects were measured.

FIGURE 18

Map of Challicum wind farm and transmitter location

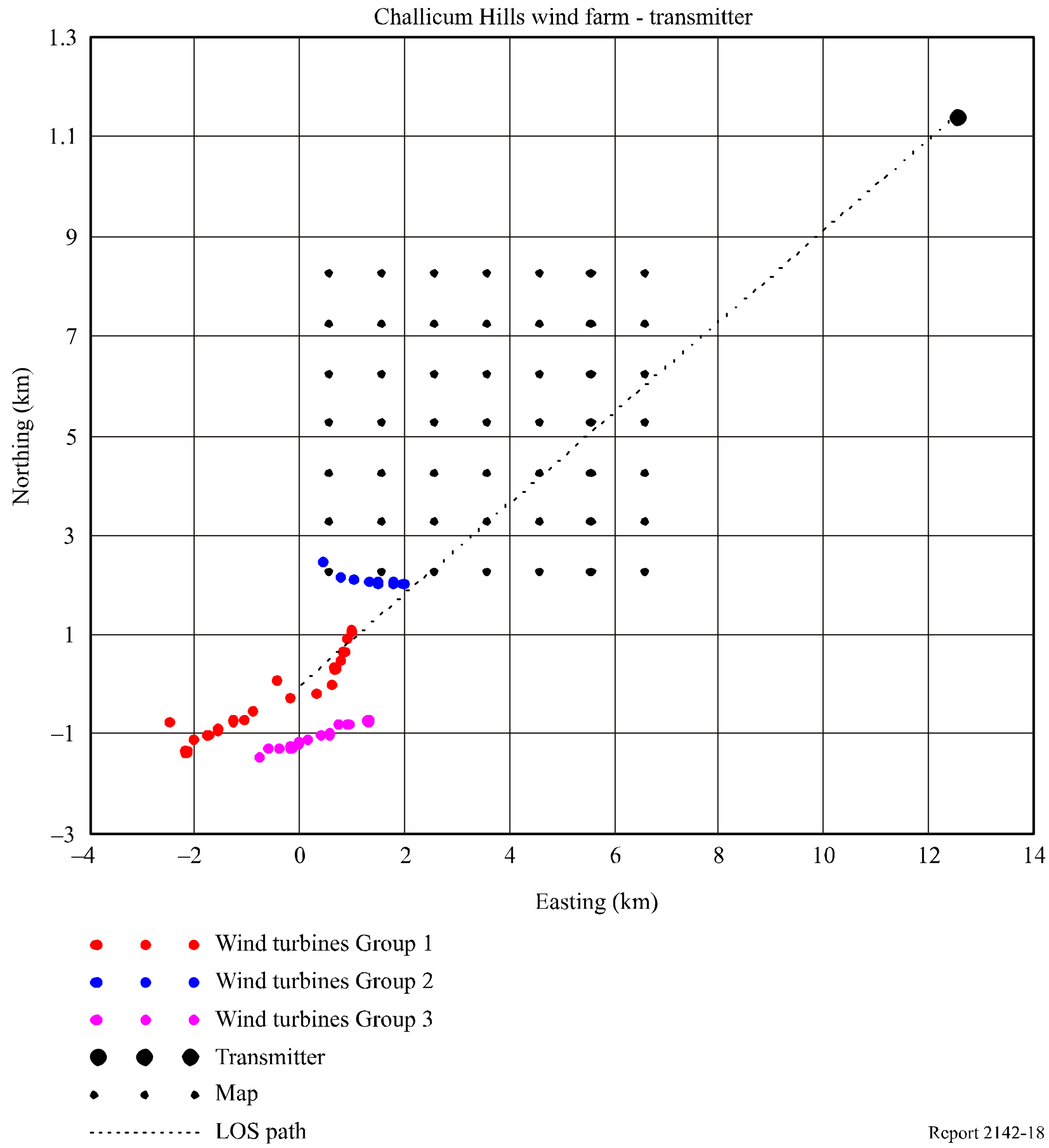

Figure 18 also shows the geographic relationship between the wind farm and the nearby television transmitters. The distance to the transmitter is between 14 and 20 km. The altitude of the transmitting antenna is about 1 150 m, or about 700 m above the mean altitude of the wind turbine rotors. In Fig. 18, the straight line joins the transmitter to the centre of the wind farm; backscattering from the pylons is expected to be dominant near this line. The incident signal subtends an angle of about 2.4º above the horizon at the wind farm. As the pylons are tapered by about 1.2º, the corresponding reflections are at about 1.2º below the horizon, and intersect the surrounding land a few kilometres from the wind turbine.

The origin (0, 0) in the map is the mean of the grid coordinates of the 35 wind turbines. The black dots show where the interference map of § 2.3 was computed. The dotted line is from the transmitter to the centre of the wind farm.

2.3 Predicted interference map from pylon scattering

The scattering coefficient from the pylons was calculated (as described in Annex 1) using geographic information for the wind farm and transmitter, and an interference map was produced covering the area between the wind farm and the transmitter, where the strongest scattering is expected.

Due to local terrain, the turbines further away from the transmitter (Groups 1 and 3 in Fig. 18) are somewhat shielded by the closer ridge where Group 2 is located. A rigorous calculation of scattering would include diffraction losses over this ridge line. To simplify the calculations, the total interference was calculated assuming clear LoS propagation, which overestimates the scattering coefficient. The predicted scattering from the pylons is shown in Fig. 19. The peak scattering coefficient is 0.17 (or –15.4 dB) in a "hot spot" 6 km east and 6 km north of the centre of the wind farm. A similar calculation was done with only the closest seven wind turbines (Group 2). The scattering coefficient using all turbines and LoS propagation was only moderately larger than that using only the nearest group and it can be concluded that the scattering coefficient in the area between the transmitter and the wind farm is due almost entirely to the closest turbines.

It is also clear from Fig. 19 that forward scattering is small compared with the backscattering.

The maximum scattering coefficient is about 0.17 at about 6.3 km east and 5.1 km north of the wind farm central reference point. The grid is 2 km^2, based on the Australian Map Grid.

The impulse response of the multipath scattering environment can be estimated from the interference signal of each turbine. Figure 20 shows the results for 35 pylons, at the hot spot location defined above and assuming an omnidirectional receiving antenna. For actual television reception, a directional antenna with significant front-to-back ratio would be used, resulting in much lower interference. However, to measure the interference signals, an antenna with a front-to-back ratio of about 25 dB was pointed **towards** the interference. Therefore the amplitude of the strongest interference signal should be comparable with the direct signal received through the back of the antenna. This procedure thus "amplifies" the scattered signal, making more accurate measurements possible.

Figure 20 also demonstrates the large time delays of the scattered signals, up to about 60 μs, due to the round-trip distance of about 18 km between the measurement point and the most distant wind turbine. The common guard time parameter of 1/16 corresponds to 64 μs. The measurement technique using the scattered pilot signals has a maximum measurable delay of 42.7 μs[3], and could not determine the large scattered signal delays for this case.

---

[3] This value is related to the pilot separation frequency of about 12 kHz. As the maximum Nyquist "frequency" is half of 1/12 kHz, the maximum time delay is about 1/24 ms.

FIGURE 19

Map of the scattering from the all pylons (red dots)

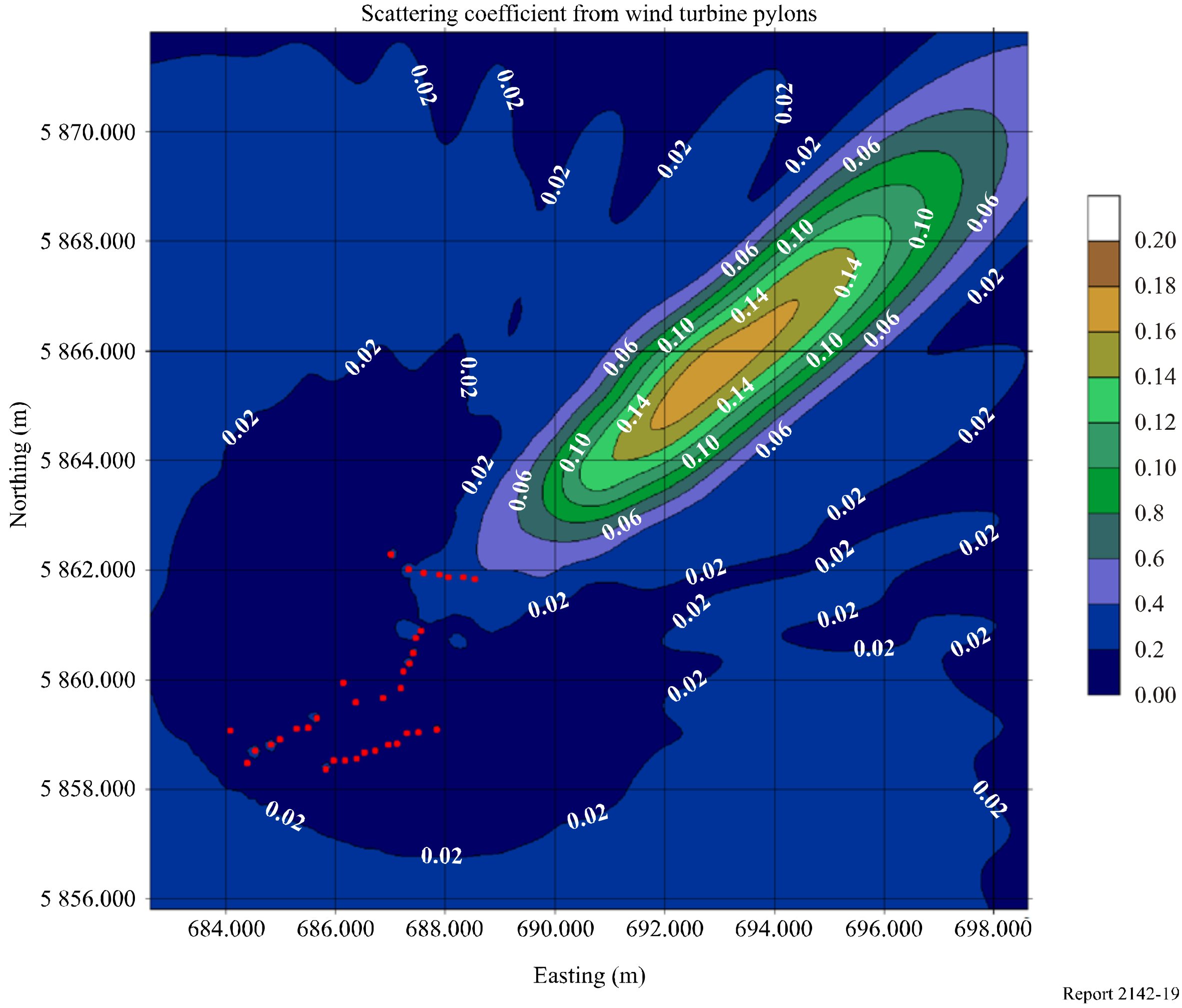

Report 2142-19

FIGURE 20

Computed multipath impulse response for the scattering from all 35 wind turbine pylons at the interference hot spot location

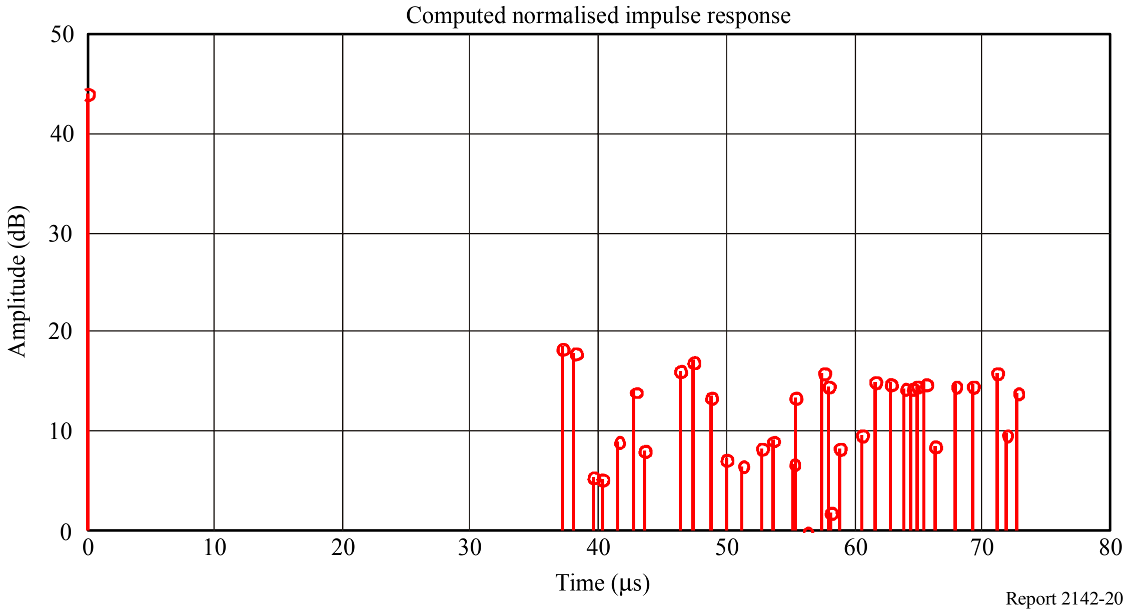

Report 2142-20

The direct signal is also shown at 0 μs. An omnidirectional antenna was assumed. The data are normalized so that the weakest signal from a wind turbine is 0 dB.

2.4 Predicted interference map from blade scattering

The calculation of the scattering from the turbine blades is similar to that from the pylons, but with two complicating factors. First, the rotation of the blades produces a scattering pattern which varies cyclically about every two seconds. Secondly, the axis of the rotor in the horizontal plane changes with the wind direction. Maximum scattering occurs when the wind direction is aligned with the line from the transmitter to the wind farm (see Fig. 18), that is, when the wind direction is in the NE-SW direction[4]. The problem is further complicated by the fact that there are many independently operating wind turbines in a wind farm, so a deterministic solution for one particular orientation of the blades on each turbine is not useful for planning purposes.

To calculate the scattering from the blades, therefore, a wind direction is assumed, and it is assumed that the plane of the blades are all orientated normal to this direction. As the rotation angles of the turbines are unsynchronized, it is assumed that the angles are distributed with a uniform random distribution in the range 0º to 360º. Because all the turbines rotate at the same rate, these angle distributions remain constant. The scattering coefficient at each point in the map was calculated as the average scattering coefficient with this random offset angle for each wind turbine. The maps therefore represent a statistical average of the scattering, with the dynamic variations ignored. Because the blades rotate only a very small angle[5] during the OFDM symbol period of about 1 ms, the scattering can be considered as quasi-stationary. The scattering coefficient itself is a statistical parameter describing (approximately) a Rayleigh distributed signal amplitude, or a Ricean distributed signal amplitude is the direct signal is included.

As the blades rotate, the scattered signal received at a point will vary in a cyclical fashion. An example is shown in Fig. 21, illustrating the variation at "hot spot" from Fig. 19. Scattering from all 35 turbines was calculated with the simplifying assumption of LoS propagation and all rotors oriented normal to the wind direction. Despite the complexity, a fundamental component at one-third the rotation period is clear. The scattered signal varies by a factor of about 2.25.

The relative angular positions of the rotors on each turbine were selected randomly. The scattering coefficient was computed at the position of maximum scattering shown in Fig. 19.

In predicting scattering over a geographic area, the statistical approach described above will be used, ignoring the time-varying nature of the scattering. The resulting map with the wind direction NE-SW (worst case), based on all 35 turbines and with no diffraction loss, is shown in Fig. 22. An omnidirectional antenna is assumed, and the material reflection coefficient is assumed to be unity. As the blades are not metallic, a more realistic material reflection coefficient would be about 0.5. With these assumptions, the maps are will overestimate the scattering coefficient.

Figure 22 shows that, for the blades as for the pylons described earlier, the backscattering is largely confined to a narrow beam along the line from the transmitter to the wind farm. The position of maximum interference is 5.5 km NE of the centre of the wind farm. The interference in the forward scatter direction is much less than in the backscatter direction. The scattering coefficient map has a complex spatial distribution. Although not visible in this version of the plot, the interference "hot spot" has a value of 0.11 and is confined to a narrow region a few hundred metres long.

---

[4] If the small blocking effect of the pylon is ignored, then the scattering geometry is symmetrical about two directions 180º apart. The small axial rotation of the blade is ignored in this analysis.

[5] With a rotation period of 2 s, the angular rotation during an OFDM symbol period is 0.18º.

FIGURE 21

Calculated scattering coefficient variation from 35 turbines for the period of one rotation of the rotor

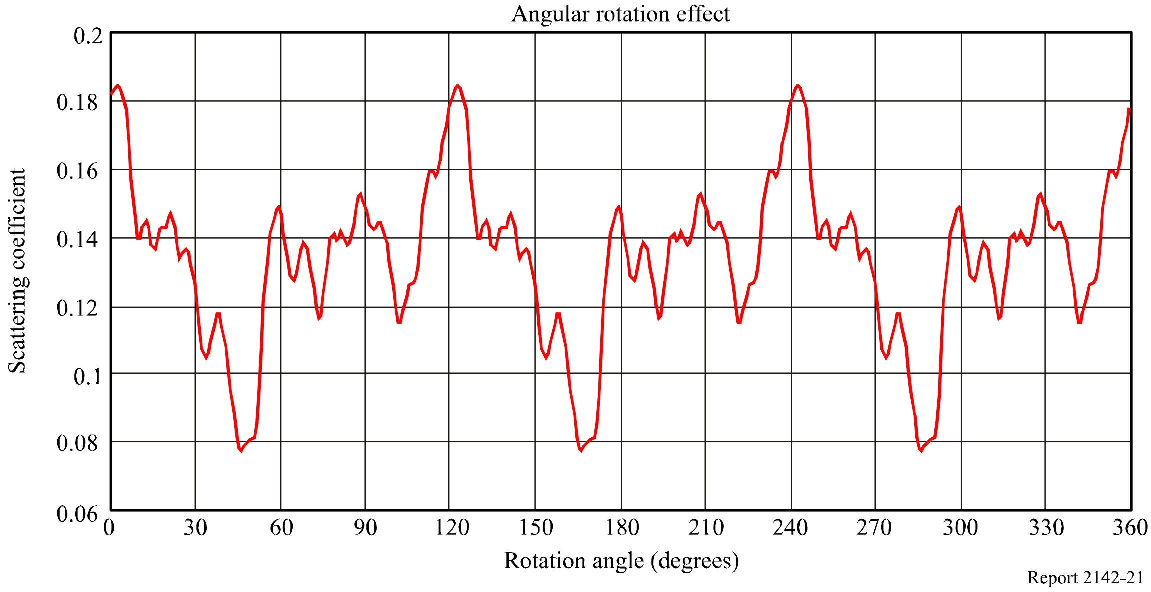

Report 2142-21

FIGURE 22

Calculated scattering coefficient from the blades of 35 wind turbines (red dots)

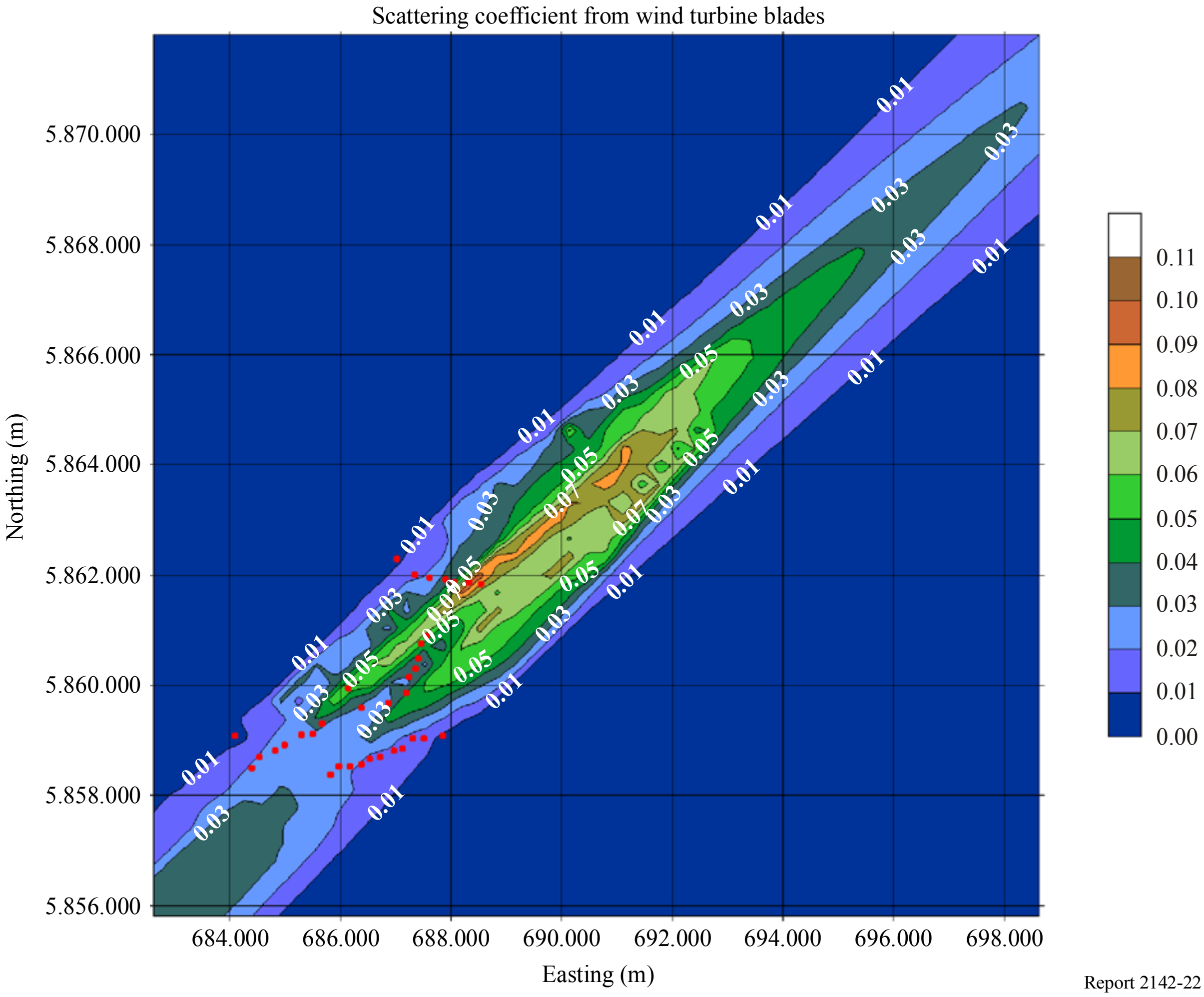

Report 2142-22

The wind direction is SW-NE, approximately along the line from the transmitter to the wind farm, which results in worst-case interference. The rotor rotation angle is assumed to be a random variable with uniform distribution. The peak scattering coefficient is about 0.11. The grid size is 2 000 m.

The calculated scattering coefficients for other wind directions are shown in Figs. 23 and 24. In Fig. 23 the wind direction is N-S, and the backscattered and forward-scattered signals are approximately at right angles. As the incident signal is not normal to the blades, the peak value of the interference signal is somewhat less (0.08 compared with 0.11) than in Fig. 22, but the backscattered signal is still much greater than the forward-scattered signal.

Figure 24 represents scattering when the wind direction is SE-NW and blades are edge-on to the incident signal. The scattering is quite small, confined to a region close to the wind farm, and approximately omnidirectional. However, the effect of the motion of the blades should be considered. The speed at the tip of the blades is of the order of 100 m/s, and the associated Doppler frequency for an RF frequency of 600 MHz is ±200 Hz. As the OFDM signal tone spacing is about 1 000 Hz, the scattered signal could result in appreciable spectral widening, with consequential effects on the digital television receiver decoding performance. However, as the magnitude of the scattered signal is low, this effect should be relatively small.

FIGURE 23

Calculated scattering coefficient from the blades of 35 wind turbines (red dots)

Scattering coefficient from wind turbine blades

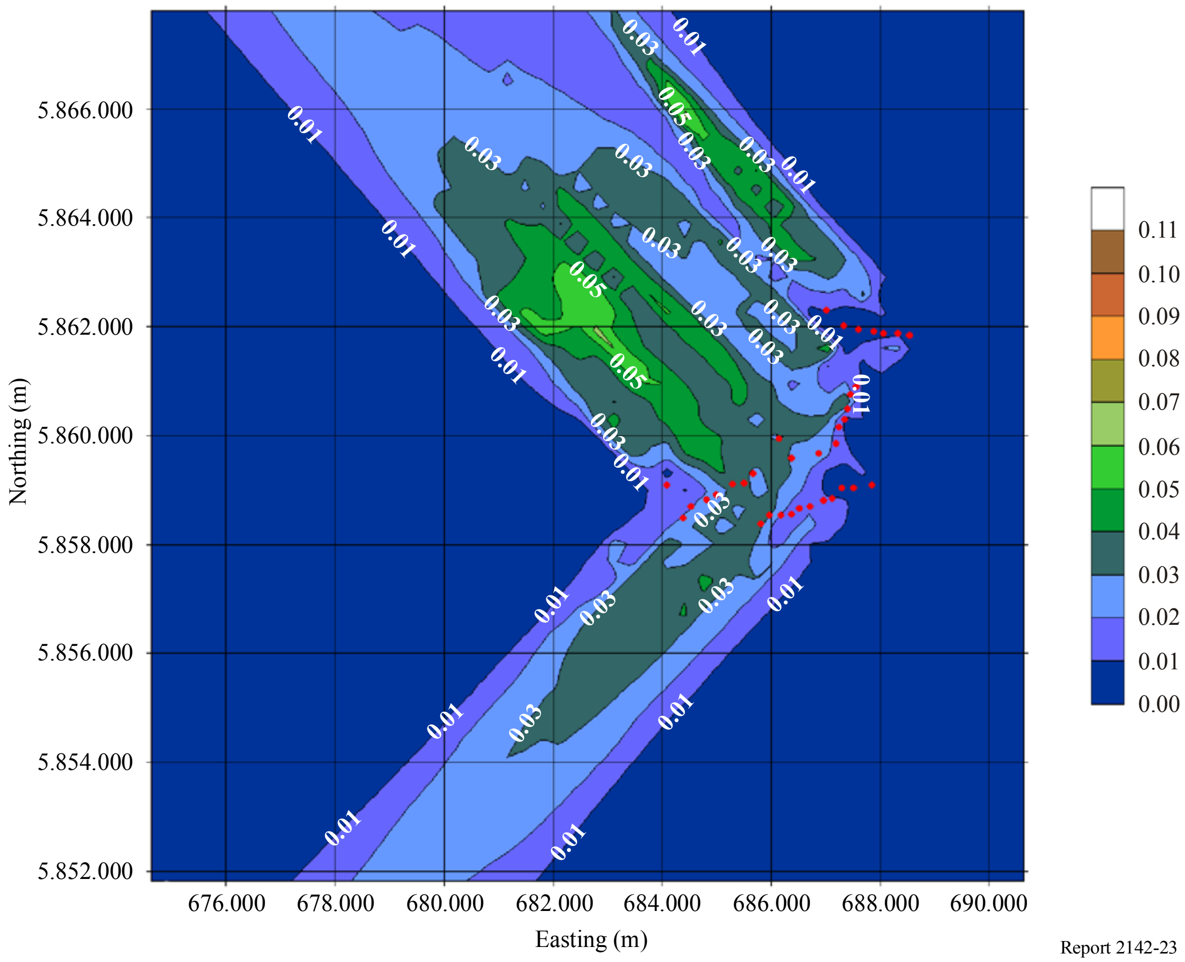

Report 2142-23

The wind direction is S-N. The rotor rotation angle is assumed to be random with uniform distribution. The peak scattering coefficient is about 0.08. The grid size is 2 000 m.

FIGURE 24

Calculated scattering coefficient from the blades of 35 wind turbines (red dots)

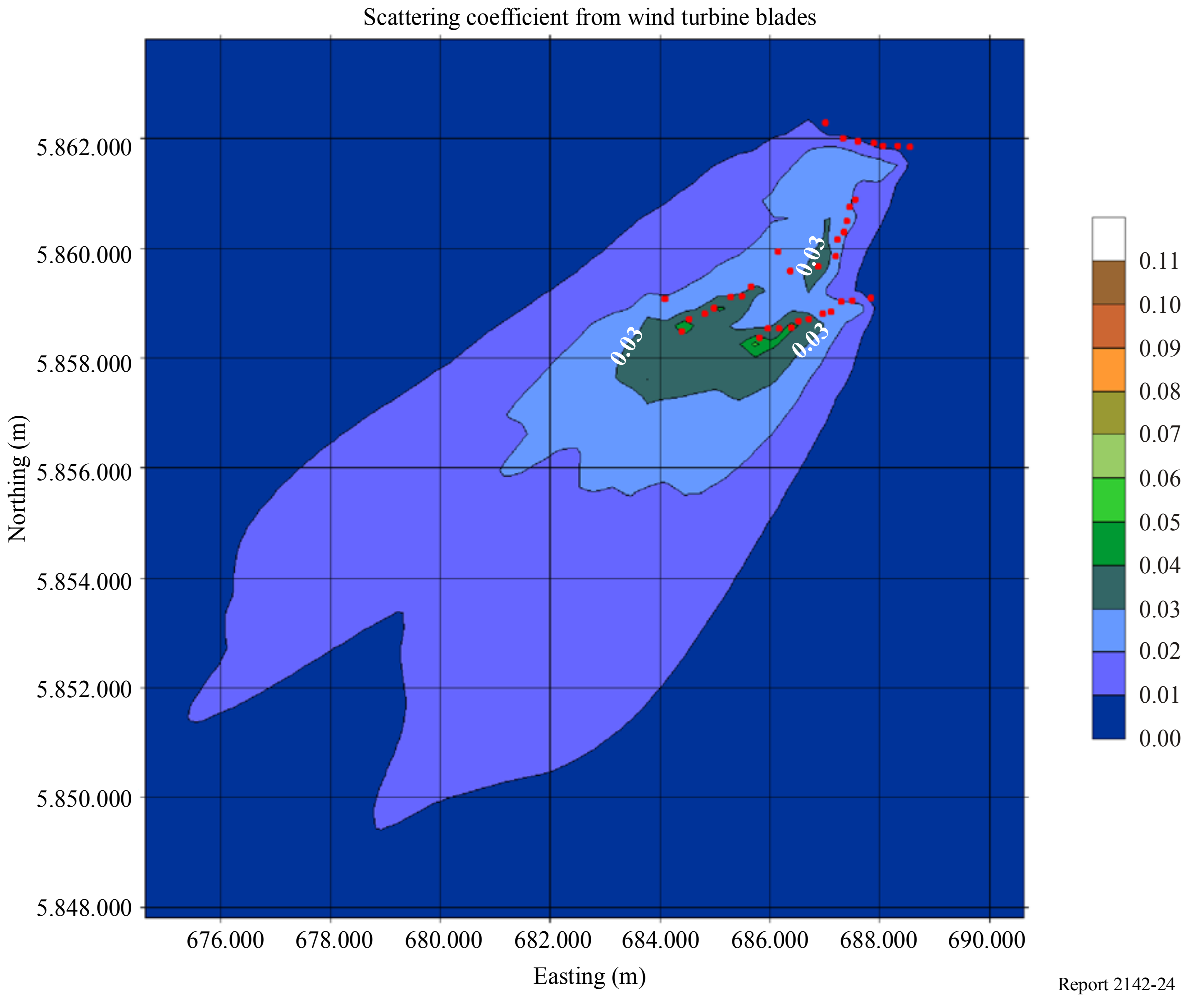

The wind direction is SE-NW, approximately normal to the line from the transmitter to the wind farm, resulting in minimum scattering of the signal, both in magnitude and geographic area. The rotor rotation angle is assumed to be random with uniform distribution. The peak scattering coefficient is about 0.06. The grid size is 2 000 m.

2.5 Predicted receiver performance

The performance of digital television receivers was assessed using methods described in Recommendation ITU-R BT.1735 – Methods for objective quality coverage assessment of digital terrestrial television broadcasting signals of System B specified in Recommendation ITU-R BT.1306. This Recommendation defines the "quality" of the receiver output in terms of the bit error rate (BER) and the signal strength. In the context of the scattering from wind turbines, the most important parameter is the BER out of the receiver demodulator, before error correction.

The BER for locations near the wind farm was estimated from the predicted impulse response. Using a good antenna, about 100 ms of signal was recorded in suburban Sydney, Australia. This received signal had low multipath corruption, with a measured modulation error ratio (MER) of about 27 dB, and a channel BER (termed CBER in Recommendation ITU-R BT.1735) of about 0.002. This reference signal was used to generate simulated signals based on the propagation impulse responses computed by the scattering simulation program.

The reference signal is shown in Figs. 25 and 26. The impulse response in Fig. 25 is largely free from multipath corruption. The computed channel BER for about 100 symbols is shown in Fig. 26 with a mean value of BER of 0.0019. As defined in Recommendation ITU-R BT.1735, satisfactory operation for a rate 2/3 Viterbi decoder requires a BER less than 0.04.

FIGURE 25

Computed impulse response of the reference signal, largely free from multipath interference

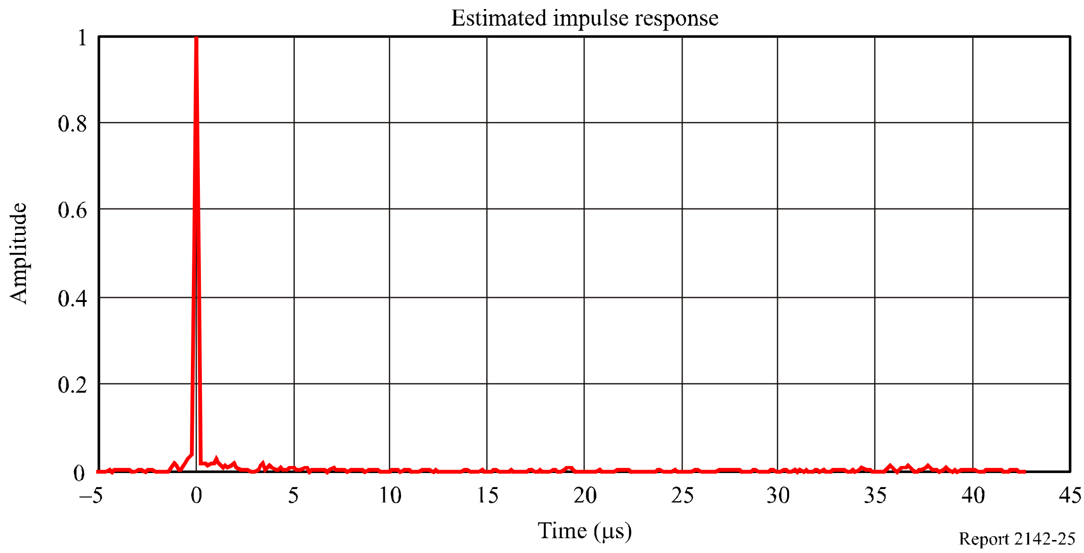

FIGURE 26

Computed channel BER for the reference signal for 96 symbols

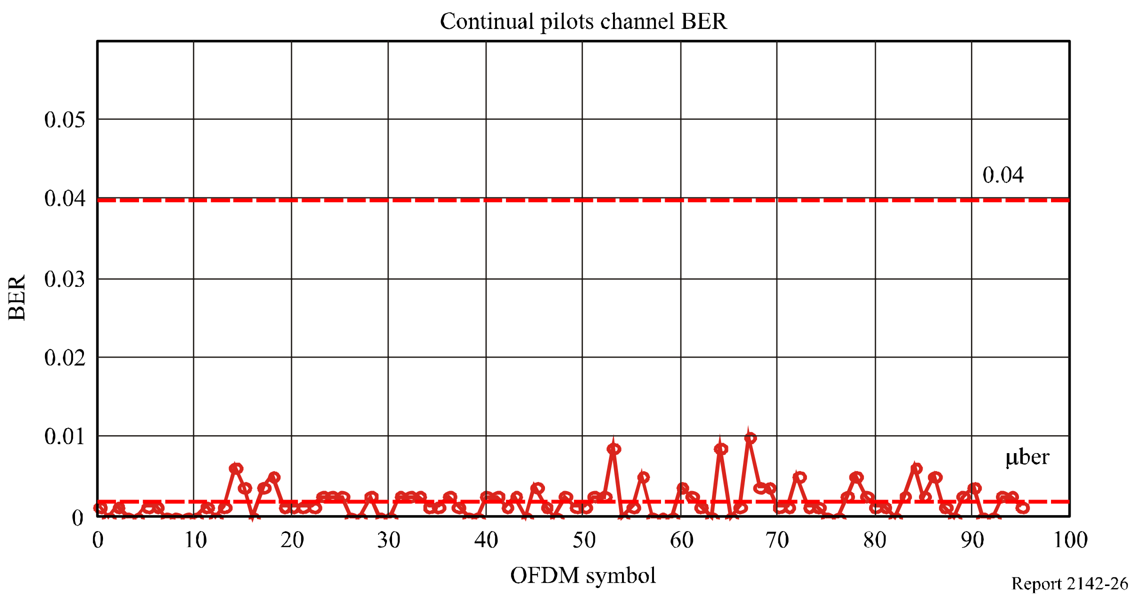

The mean BER is 0.0019, but with some symbols peaking at about 0.01. The limit for satisfactory operation is 0.04.

The same parameters were then calculated for the wind farm “hot spot” location, assuming an omnidirectional antenna. The results are shown in Figs. 27 and 28. Compared to the ideal response in Fig. 25, the impulse response of Fig. 27 has components at delays greater than about 35 µs. Figure 28 demonstrates that the BER is significantly degraded relative to the reference signal, and the BER is well above the acceptance limit of 0.04, so digital television reception would not be possible. However, the calculations assumed an omnidirectional antenna, and considerable improvement would result from an antenna with a good front-to-back ratio.

FIGURE 27

Computed impulse response at the Challicum Hills “hot spot” with scattering from 35 wind turbines (pylons and blades)

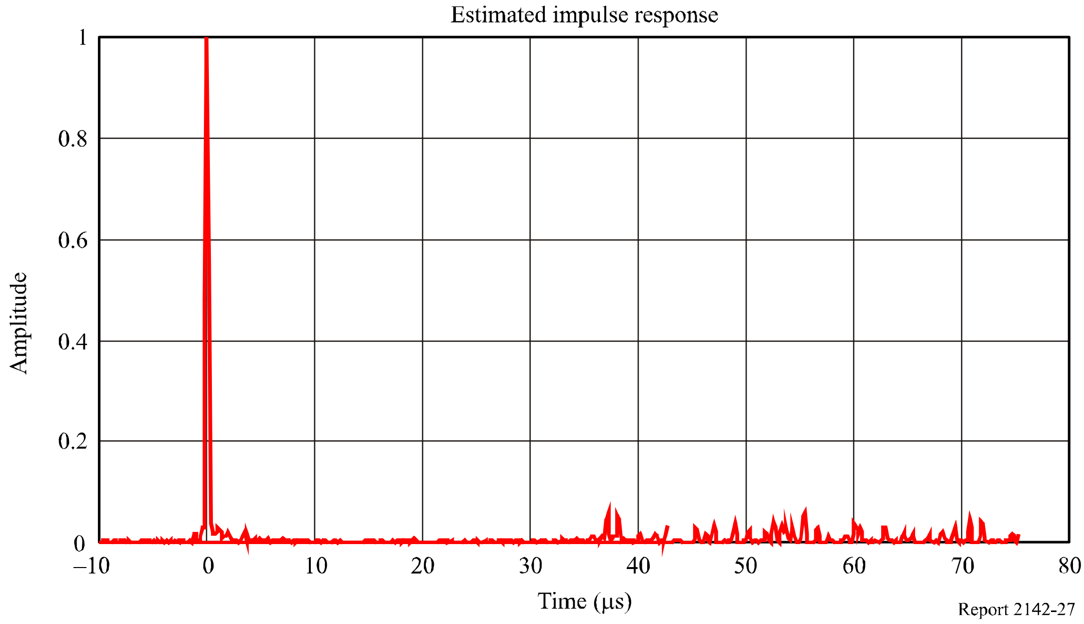

The receiving antenna is omnidirectional. The peak multipath interference occurs at about 35 µs delay, and has a value of about –23 dB.

The mean BER is about 0.123, far above the acceptable limit of 0.04.

Figures 25 to 28 were calculated with an omnidirectional antenna, but by changing the assumed antenna gain, the performance of the receiver over a range of operating conditions can be estimated. The results are summarized in Figs. 29 and 30.

Figure 29 shows the effect of the scattering coefficient on the channel BER. At the BER of 0.04 (satisfactory performance), the allowable scattering coefficient is about –21.5 dB.

The effect of the scattering coefficient on the signal modulation error ratio (MER) at the “hot spot” is shown in Fig. 30. Based on the scattering coefficient of –21.5 dB, the limiting MER for satisfactory operation is 21 dB.

While the results summarized in Figs. 29 and 30 are for a specific receiver performance, due to the random processes[6] involved, it is expected that these results can be applied to the general case. If the scattering coefficient (at the output of the antenna) can be measured or calculated,

[6] The multipath signal is the sum of a large number of random scattering processes. The statistics are approximately Gaussian with the single defining parameter being the scattering coefficient.

the performance of the receiver can be determined from these figures. The importance of the antenna gain and the scattering geometry is clearly evident, as the scattering coefficient can be affected by 10 dB or more by the antenna directivity.

FIGURE 28

Computed channel BER at the Challicum Hills "hot spot" with scattering from the 35 wind turbines (pylons and blades)

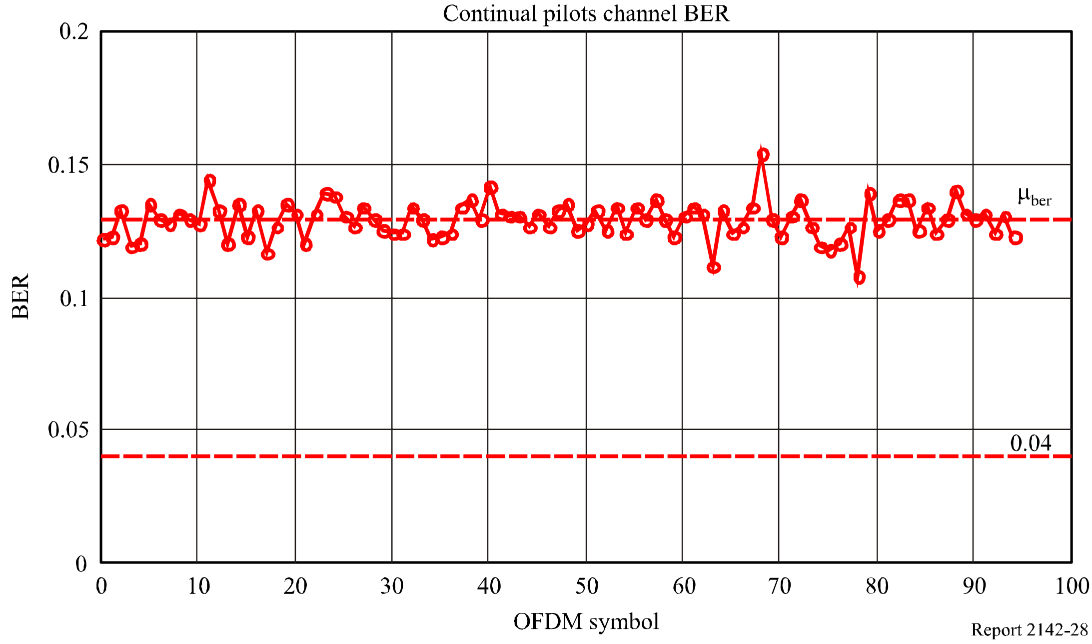

FIGURE 29

Computed channel BER at the Challicum Hills "hot spot" with scattering from the 35 wind turbines (pylons and blades) as a function of the scattering coefficient

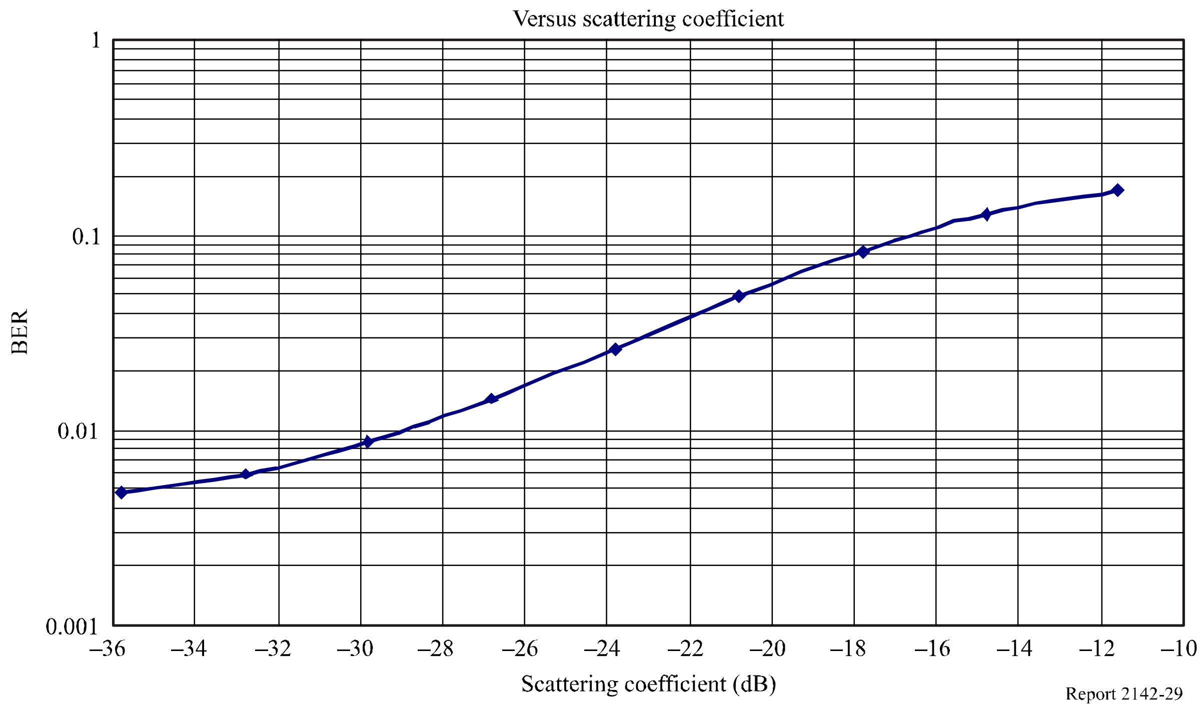

The limiting BER for satisfactory operation of the receiver is 0.04, so the limiting scattering coefficient is about 21.5 dB.

FIGURE 30

Computed channel MER at the Challicum Hills "hot spot" with scattering from the wind turbine pylons as a function of the scattering coefficient

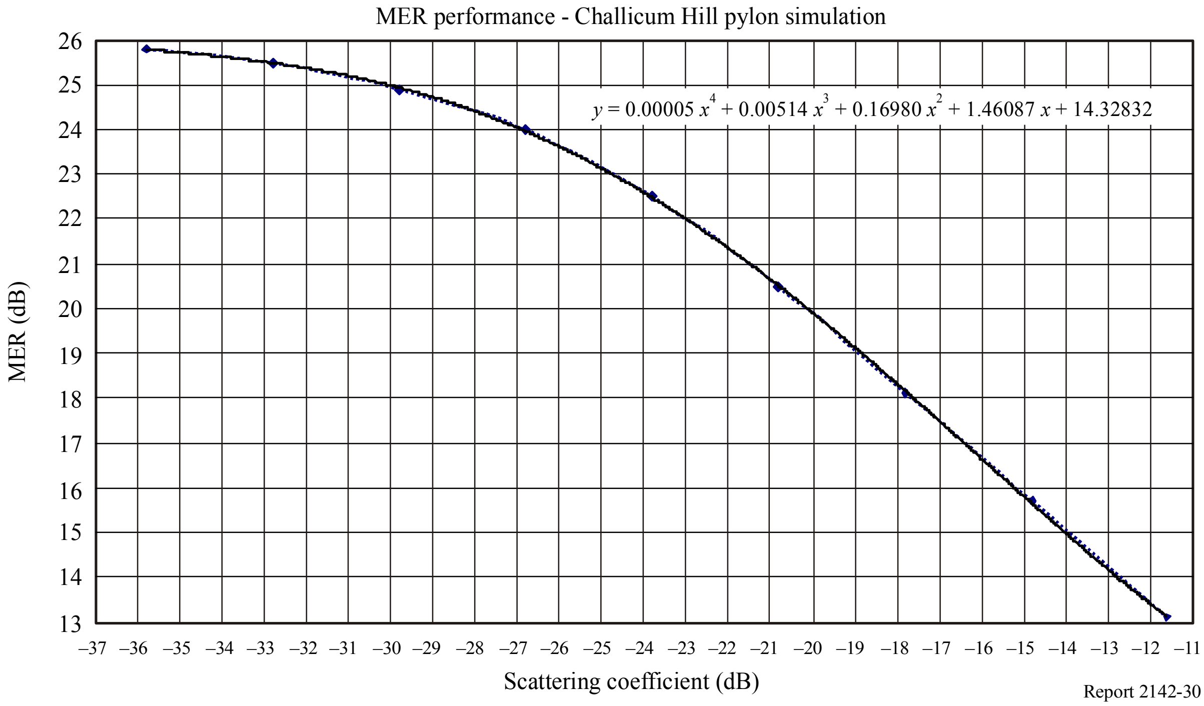

The MER curve is fitted with a fourth-order polynomial, which can be used to estimate the MER from the scattering coefficient (or vice versa).

In Fig. 31 the scattering coefficient from the pylons and the blades together was converted to prediction of MER using the relationship in Fig. 30. Similarly, Fig. 29 could be used to convert the scattering coefficient map to a CBER map. Assuming an omnidirectional receiving antenna, the minimum MER in Fig. 31 is 18.2 dB. As the minimum acceptable MER is 21.5 dB, the areas of blue and dark green, in the backscatter direction, would have unsatisfactory reception with an omnidirectional antenna. Locations for measurements, as described in § 3, were chosen by overlaying Fig. 30 on a map of the local terrain.

Scattering from the blades assumes a material reflection coefficient of 0.5. The wind direction is SW-NE (worst case).

3 Measurement results

3.1 Overview

Measurements were made in the area surrounding the wind farm, both in the forward scattering and the backscattering regions, at locations where interference was expected. As described in § 2, at any given point, scattering from the pylons is constant, but scattering from the blades depends on the wind direction. The wind directions during the measurements were such that the blade scattering region was generally in a different direction from that from the pylons, so the worst-case scenario could not be measured. For all but one location, the interference was mainly from the pylons.

However, one location did include scattering from the blades, where the scattered signal varied quite rapidly in time which could significantly affect the performance of digital television receivers.

Section 3.2 provides results from a measurement with a single interference source. Section 3.3 gives the results of the dynamic interference from the rotating blades, including the time variation of the signal. Section 3.4 provides details of the measured impulse response compared with predictions. Finally, § 3.5 provides results relating to the effects of ground reflections on the reception of the digital television signals.

FIGURE 31

Computed MER map for the wind farm (blue dots) for scattering from the wind turbine pylons and blades

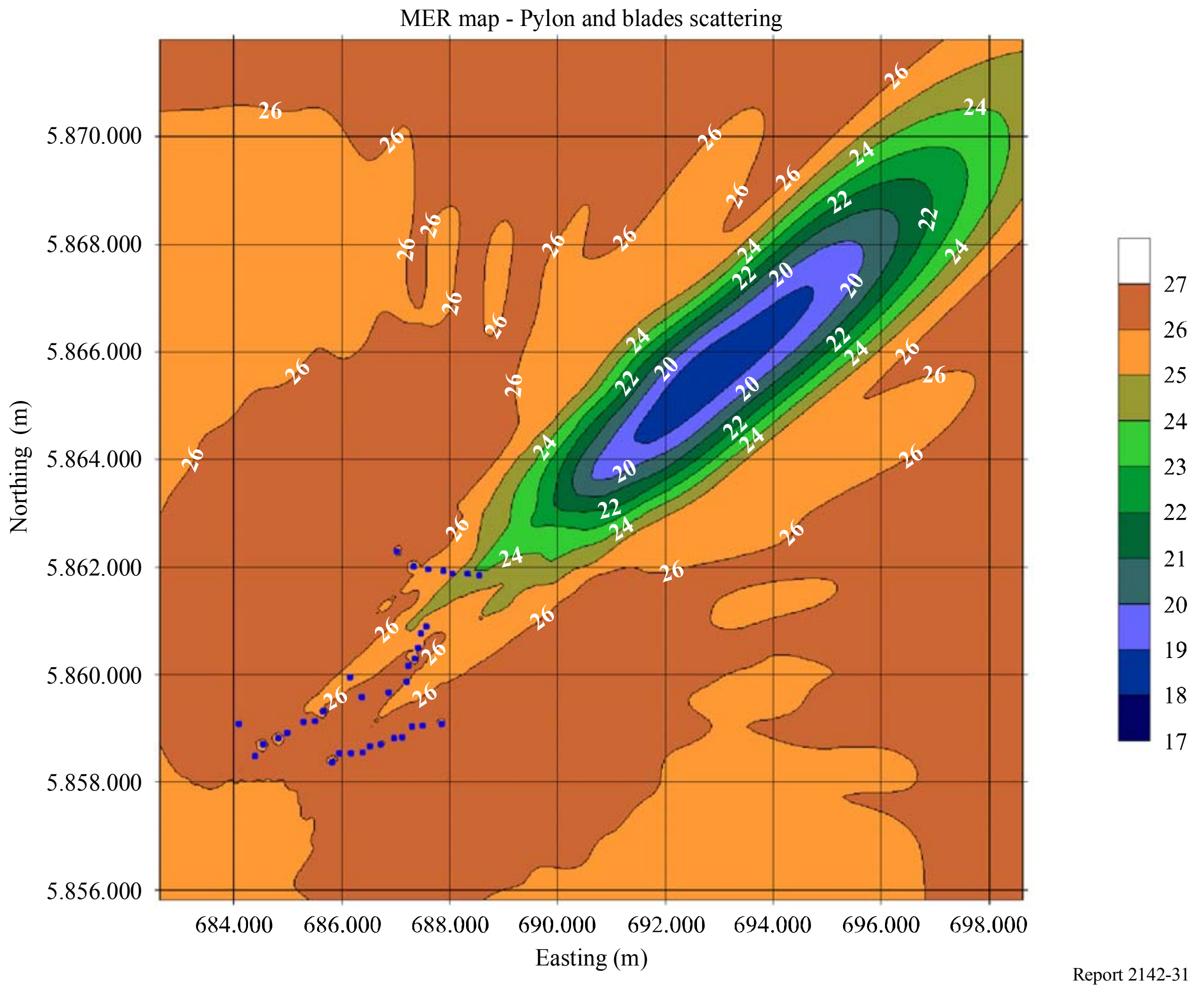

Report 2142-31

3.2 Measurement with single multipath component scattering

The first measurement location was originally chosen to obtain a reference signal, but the measured data show evidence of a single interference source. The measurement point was some distance from the wind farm, although visually LoS to almost all the wind turbines, and had a clear LoS to the transmitter. It was in an open area away from other interference objects such as trees and hills. However, the measurements show the presence of a significant multipath signal which potentially could degrade the reception performance.

The averaged spectrum of the channel is shown in Fig. 32. The data are measured at the receiver IF output which has a nominal frequency of 32/7 MHz. The maximum frequency is half the sampling rate of 20 Msample/s. The two spikes below 1.2 MHz are associated with an adjacent (analogue) TV channel. The slow slope across the channel is believed to be an artefact of the transmitted signal.

The averaged spectrum clearly shows the 64-QAM data and the larger pilot signals. The nominal shape of the spectrum should be a constant amplitude across the channel, but this measurement shows an approximately sinusoidal component with a period of about 550 kHz. This spectral shape indicates a single interference source, with the sinusoidal amplitude being the relative amplitude of the multipath signal, and the reciprocal of the spectral period being the multipath delay. In this case the relative amplitude of the multipath signal is about 0.1, and the delay is 1/0.55 = 1.8 μs. The average signal-to-noise ratio is 28 dB, which is typical of the maximum SNR from the receiver.

FIGURE 32

Measured spectrum of channel averaged over 500 symbols

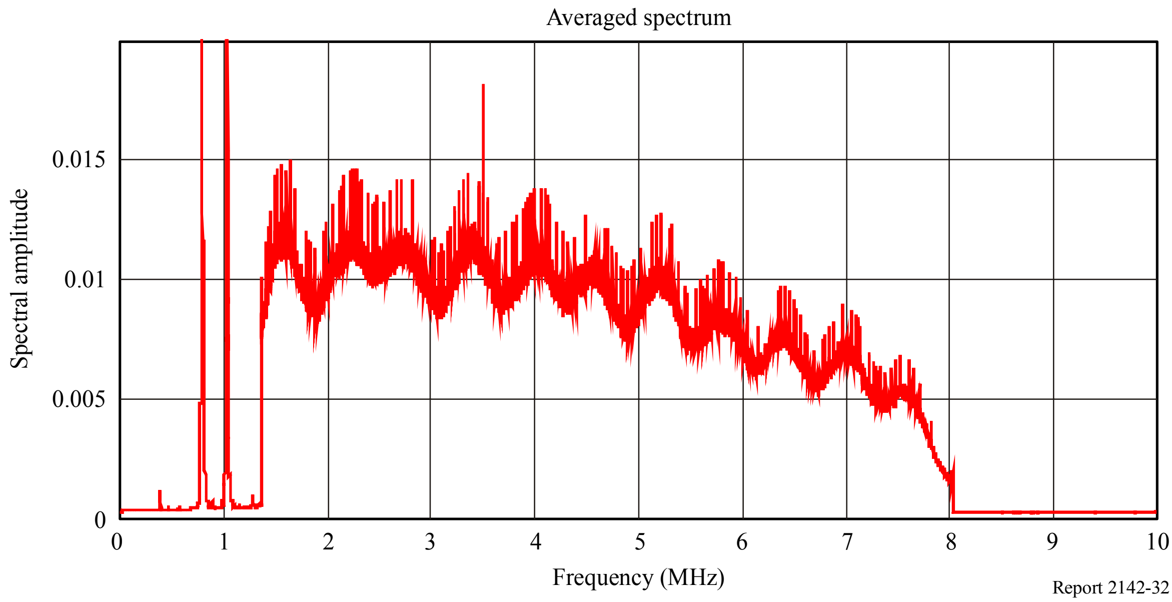

The amplitude scale is arbitrary, as the equipment does not measure absolute signal strength.

Figure 33 shows the calculated impulse response from the measured spectrum. The multipath signal is essentially confined to a single interference source with a delay of 1.65 μs and a relative amplitude of 0.1. These results agree with those derived from the spectrum, but are more accurate as the spectral data has more "noise" due to the 64-QAM data modulation. While the two methods result in similar conclusions, the impulse response method is preferred.

Calculated impulse response for the spectrum shown in Fig. 32. The relative amplitude is 0.1 (–20 dB), and the multipath delay is 1.65 μs. The measurement time resolution is 0.3 μs.

As the receiver is located in an open area, the multipath interference is most likely located at the transmitter end. The most probable location for the interference source is a ridge about 2 km from the transmitter along the propagation path.

FIGURE 33

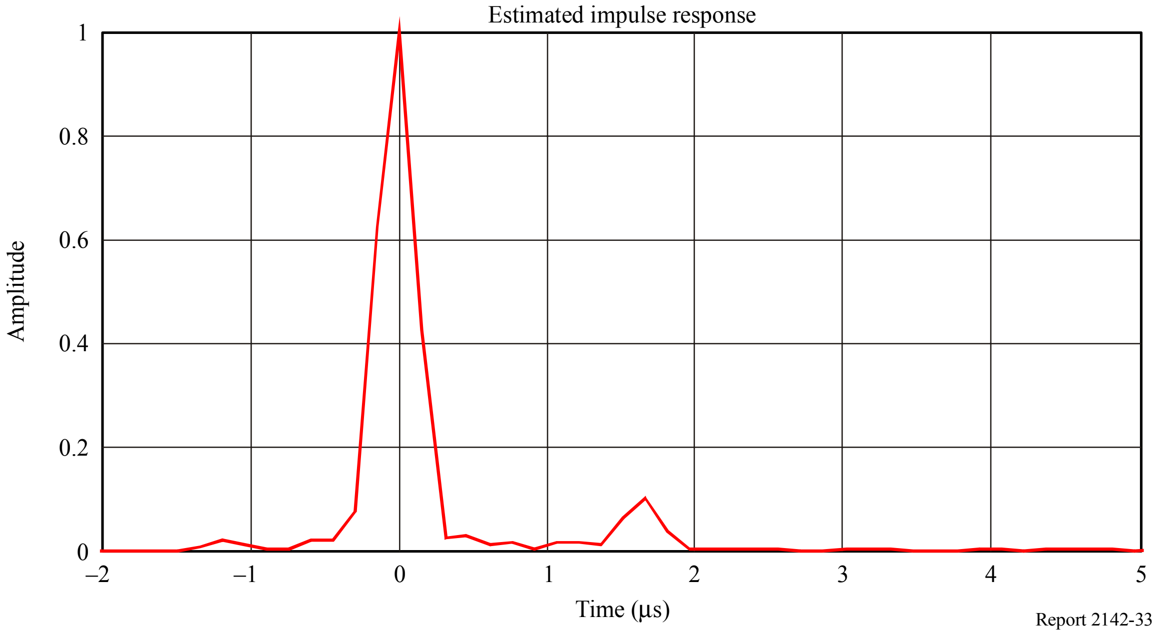

The signal spectrum variation due to multipath signals can be corrected in the receiver by using the scattered pilot signals as a reference. Residual errors after this correction are random due to receiver noise and are not due to the multipath interference. The measure of this noise can be expressed as the Ricean factor (ratio of the signal power to the noise power). The Ricean factor is closely related to the MER typically used for digital television quality specification. In this case it is calculated as 26 dB, and the associated 64-QAM MER is 24.6 dB. This relatively poor MER performance is due to the phase noise in the receiver rather than the signal itself.

3.3 Dynamic interference signal performance

A second example is taken from a site which was close to four wind turbines, where the direct signal was blocked by nearby hills and therefore reduced by about 30 dB. Consequently, the signal-to-interference ratio was considerably reduced, making the variation in the signal large relative to the direct signal. Further, the wind direction was such that the reflections from the blades (from one wind turbine in particular) were directed towards the receiver.

The measurements at this point are shown in Figs. 34 to 38. The parameters were calculated every fourth symbol (approximately every 4 ms). The dynamic effects due to the rotating blades result in time variations on the time scale of the order of 10-50 ms. All the data are based on a transmission with a 1/8 guard period, which is sufficient to ensure there is no inter-symbol interference.

The variation in the signal SNR (based on the guard period and the corresponding section of the useful part of the symbol) and the Ricean factor (derived from the impulse response) is shown in Fig. 34. The pattern is complex due to the scattering from more than one wind turbine. The main feature is the sharp drop in the SNR/Ricean factor, which occurs at about a 1 s period, which is the period of repetition for the rotating blade. Simulations suggest and these measurements confirm that when a blade is appropriately orientated, a narrow scattered beam is created. The signal magnitude can drop to a minimum then increase to a maximum in a period of about 30 ms. While this period is relatively long compared with the symbol period of about 1 ms, the performance is critically dependent on how the receiver tracks these changes.

FIGURE 34

Computed SNR and Ricean factor as a function of time at location site 8

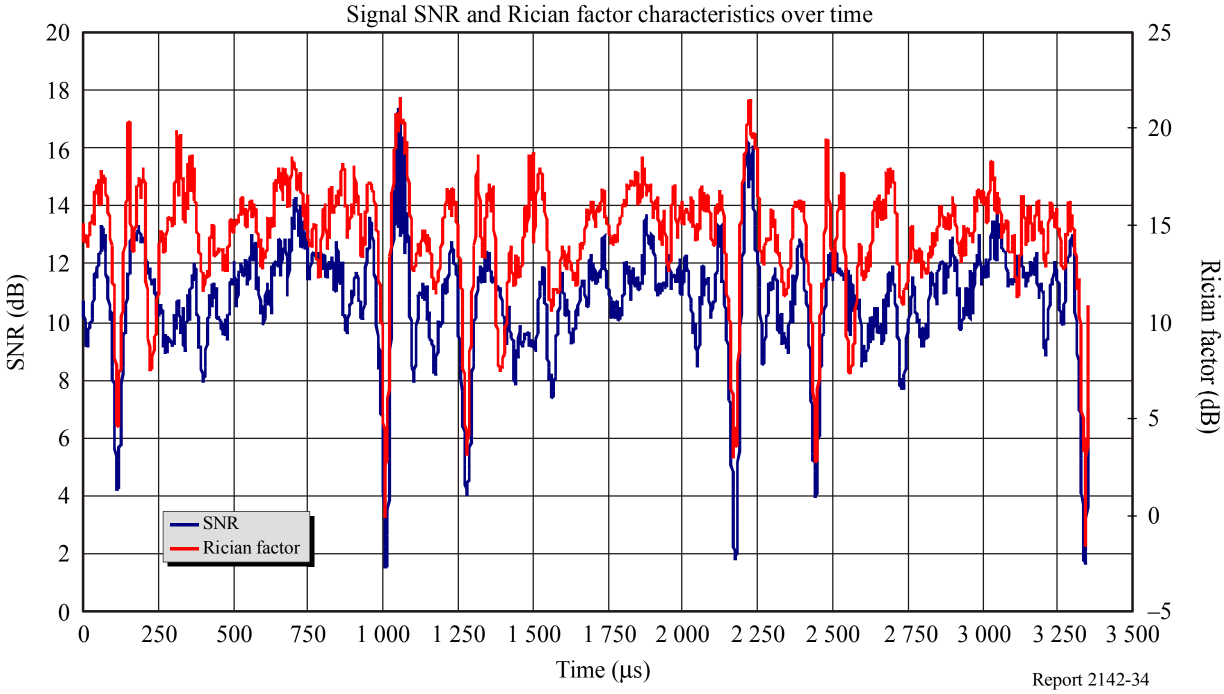

Report 2142-34

The effect on the computed frequency error is shown in Fig. 35. The frequency error is incorrectly computed when the scattered signal is large, and some form of averaging is required to avoid mistuning the receiver. In addition, the receiver tuning "noise" is increased to 21.6 Hz from the reference signal value of 15 Hz.

FIGURE 35

Computed fine tuning frequency correction as a function of the symbol number

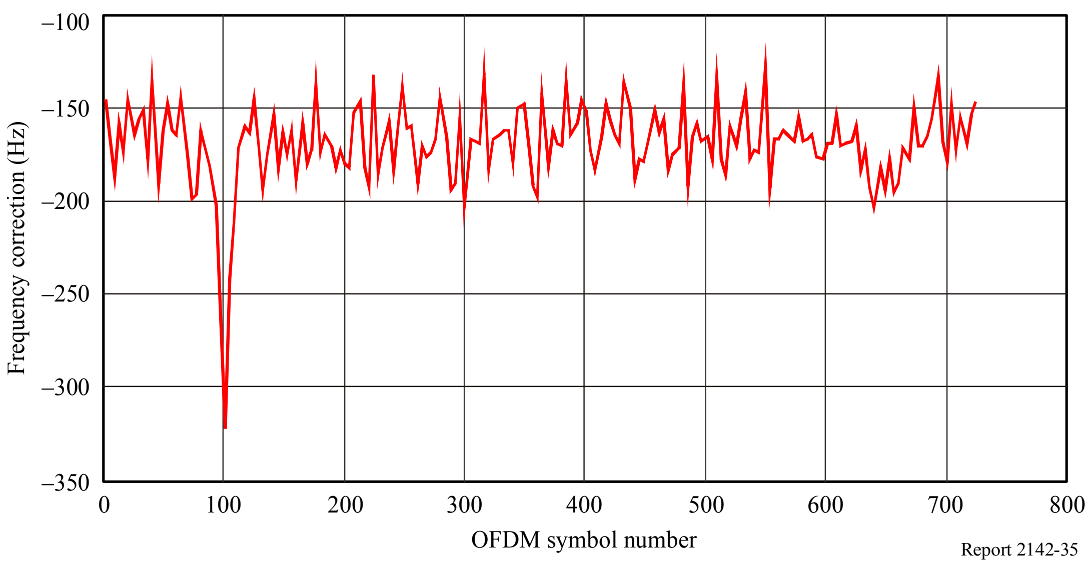

Report 2142-35

There is a large incorrect frequency error estimate at about symbol 100 due to the scattering. The frequency error noise in other symbols is a combination phase noise in the local oscillator and the effects of signal scattering. The standard deviation in the frequency estimate is 21.6°.

The effect on the measured pilot phase error is shown in Fig. 36. The interference signal causes large phase errors when the interference is maximum, but the general phase error increased from the reference level of about 2.5° (due to oscillator phase noise) to about 4° due to the interference environment.

FIGURE 36

Computed standard deviation in the continual pilots phase (using the scattered pilots as a reference) as a function of symbol number

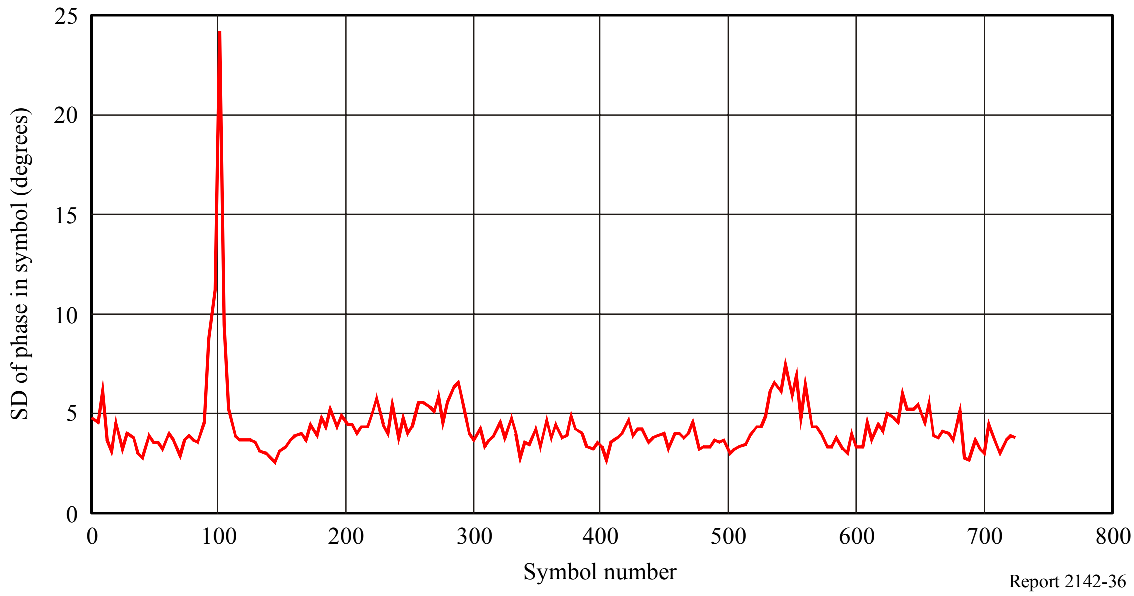

Report 2142-36

The large error at about symbol 100 and the smaller error at about symbol 550 are due to scattering.

The phase noise will limit the MER, as shown in Fig. 37. The MER decreases sharply when the interference effect is greatest, and the mean MER is also decreased to about 22 dB, a value close to the operational limit. The MER also shows slower, smaller variations which are due to scattering from rotating blades. The observed effect of the lower mean MER on the receivers was that the picture quality was variable but generally satisfactory, with occasional loss of picture and sound.

The BER as a function of time is shown in Fig. 38. This essentially mirrors the characteristics of the MER with both slow and fast variations. While the mean BER of 0.027 is satisfactory compared to the limit of 0.04, the BER frequently exceeds this value, so the characteristics of the error correcting schemes will determine the overall performance.

Overall, the received signal was considered unsatisfactory at this location. The relationship between the mean MER, the slow MER variations, the short-term MER notches and the receiver performance is not clear, but normally a MER of 22 dB should be satisfactory according to Recommendation ITU-R BT.1735. Clearly this Recommendation does not account for dynamic signal variations such as those from rotating wind turbine blades. An additional margin in the required MER should be specified when operating near wind turbines, although the magnitude of this increase has not yet been determined.

FIGURE 37

Computed MER of the scattered pilot signals as a function of time

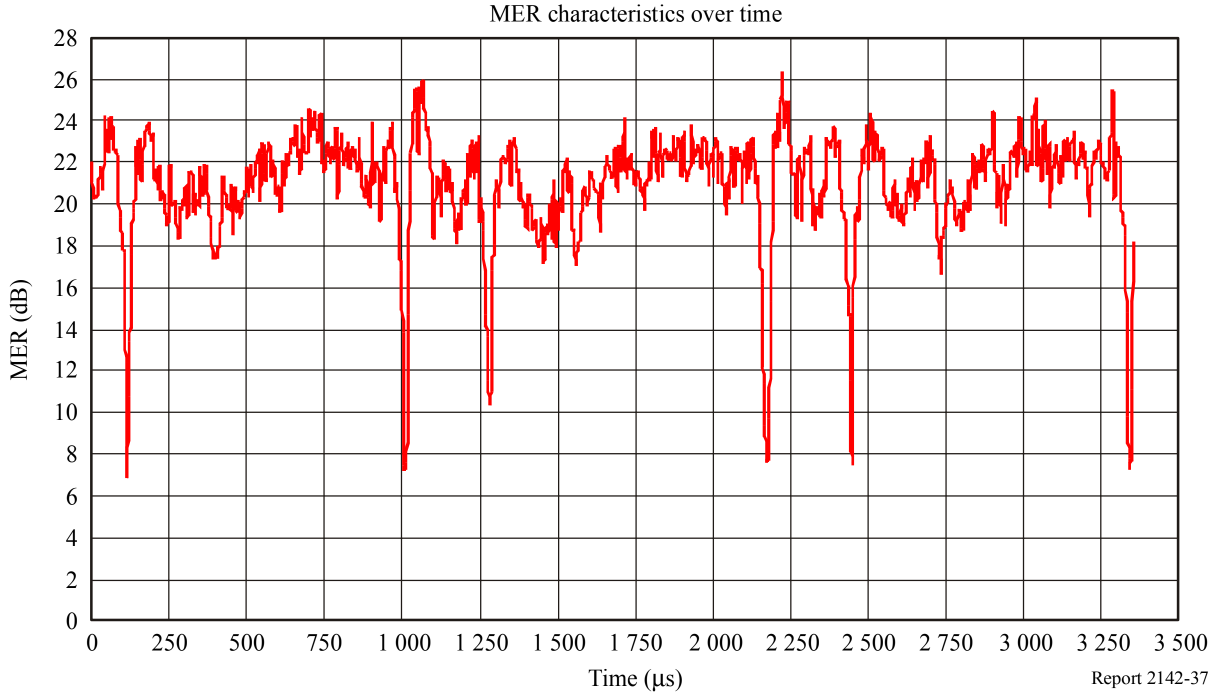

FIGURE 38

Estimate BER of 64-QAM symbols based on the scatter diagram of the continual pilots after equalization using the scattered pilots

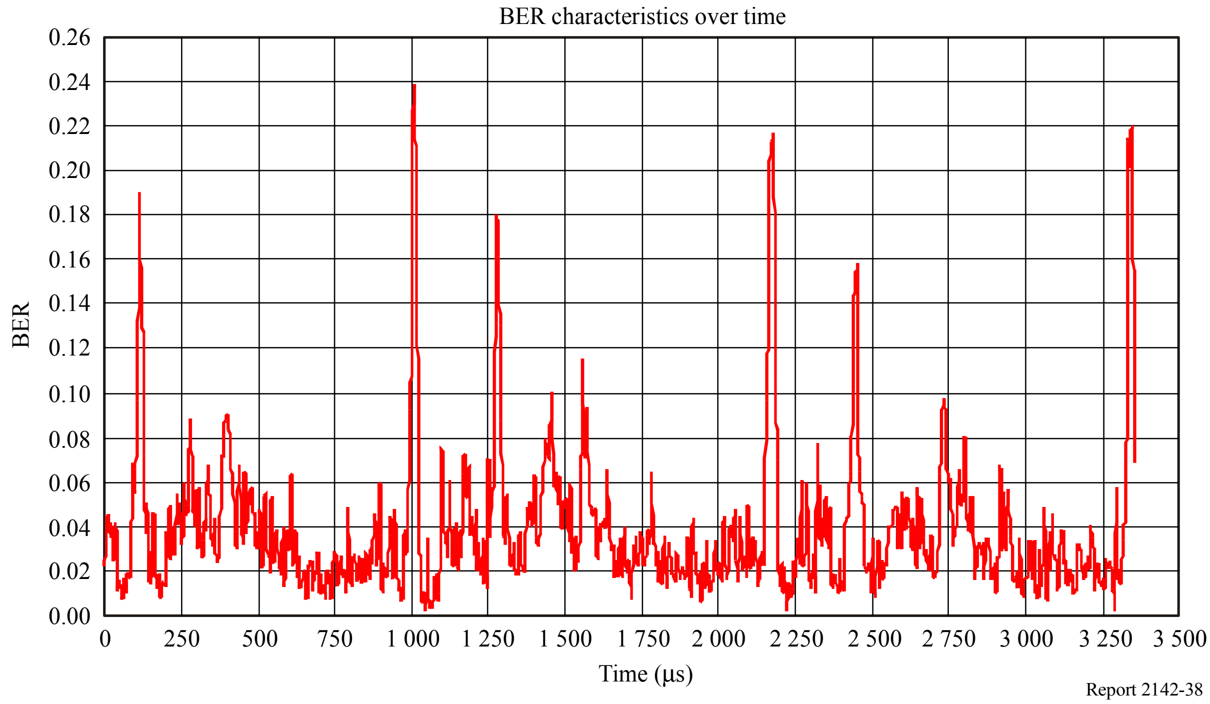

The main sections of poor performance occur at around symbols 100, 550 and 650, although there are other areas where the BER exceeds the required BER threshold for satisfactory operation. The performance was unsatisfactory as confirmed by subjective observations of the picture and sound quality.

3.4 Measured impulse response

3.4.1 Overview

As described in § 3.2, the impulse response can be calculated from the measured spectrum of the scattered pilots. With typical receiver noise, it is possible to detect interference sources 45 dB below the direct signal, with a signal-to-noise ratio of typically 10 dB.

While the impulse response method is perfectly general, the actual implementation is different for the backscattering case and the forward scattering case. The simplified geometry of these two cases is illustrated in Fig. 39. From the geometry it is easily shown that the multipath excess delay (range) for the two cases is given approximately by:

$$\Delta R \approx (1 - \cos\alpha) R \approx 0 \qquad \text{Forward}$$

$$\Delta R \approx (1 + \cos\alpha) R \approx 2R \qquad \text{Back}$$

where R is shown in Fig. 39. For the backscattering case, the main scattered component occurs at a small reflection angle α, so the delay excess is nearly twice the delay from the wind turbine to the receiver. As this distance is typically a kilometre or more, the resulting delay excess is typically greater than 10 μs in the measurements. Therefore the backscattered signals are easy to detect in the measured impulse response.

FIGURE 39

Geometry of backscattering and forward scattering from a wind turbine in relationship to the transmitter and the receiver in each case

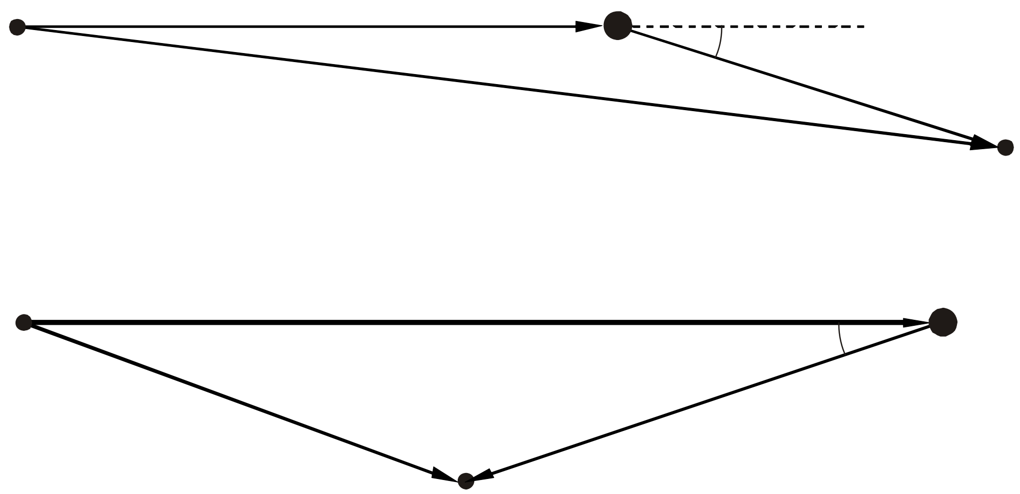

Report 2142-39

In contrast, the forward scattering occurs over a wide angle, but measurements were taken at points for which the scattering angle was relatively small. As a consequence, the delay excess is typically quite small, less than a few microseconds. The resolution of the impulse response is about 0.3 μs, due to the signal bandwidth of about 7 MHz, and therefore the multipath signals are difficult to distinguish from the direct signal.

3.4.2 Backscattering case

The measurement points for backscattering were all located near the straight line joining the wind farm to the transmitter. Figures 40 to 42 show the impulse response from three sites. The wind direction was such that minimal interference from the blades would be expected.

Measurements were made with the antenna pointing towards the wind farm and away from the transmitter, which enhanced the scattered signals relative to the direct signal by a factor equal to the antenna front-to-back ratio, about 25 dB. Even with the antenna pointing away from the transmitter, the dominant signal remains the direct signal from the transmitter. Multipath signals from terrain in the direction of the transmitter were also measured; these had an excess delay of up to 10 µs, while scattering from the wind farm had excess delays greater than 10 µs. As the measurement technique allows multipath signals to be reliably detected down to at least –45 dB, the impulse components in the following graphs indicate multipath signals rather than noise.

FIGURE 40

Impulse response at Test Point 4

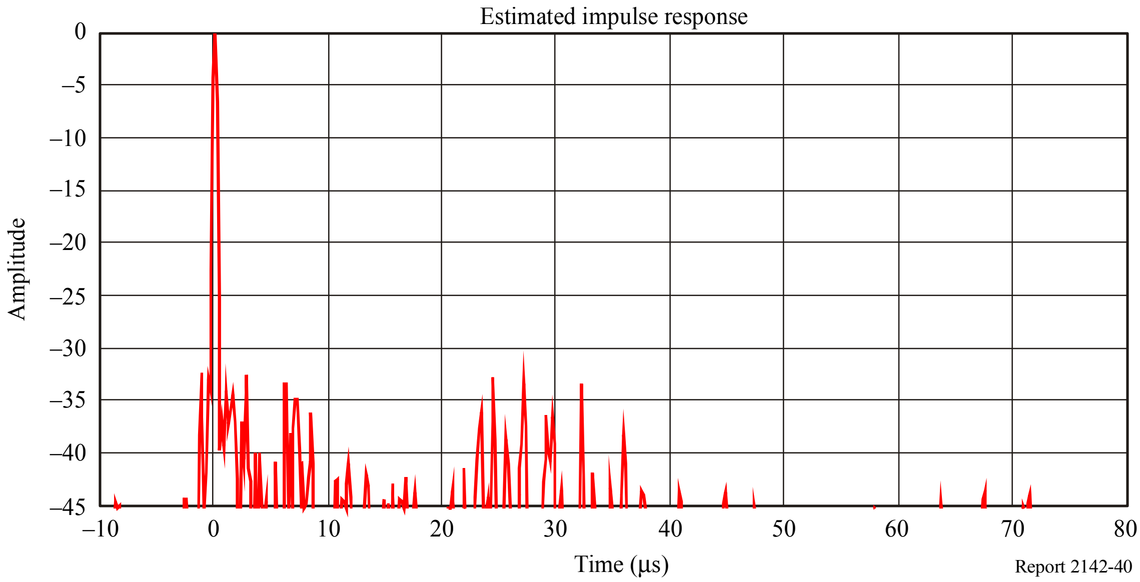

The closest wind turbine is 1.8 km, or a 10.5 µs delay. The wind turbine furthest from the measuring point (not LoS) is 7.2 km, or a 47 µs delay. The maximum scattering coefficient is –33 dB (–58 dB with an omnidirectional antenna). The wind turbines closest to the measurement point do not cause the maximum interference. Multipath signals up to 9 µs are due to terrain scattering near the transmitter. Mean BER = 0.022, and mean MER = 23 dB.

FIGURE 41

Impulse response at Test Point 5

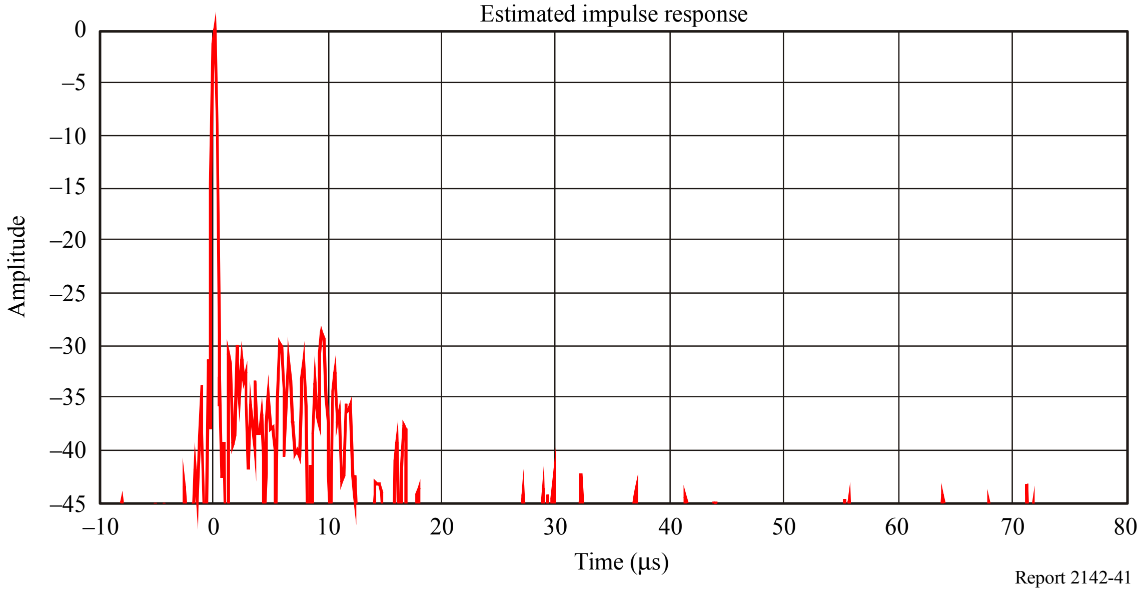

The closest wind turbine is 1.5 km (9.5 µs delay). The wind turbine furthest from the measuring point (LoS along the ridge) is 2.4 km (16 µs delay). The maximum scattering coefficient is –28 dB (–53 dB with an omnidirectional antenna). Multipath signals up to 9 µs are due to terrain scattering near the transmitter. Mean BER = 0.023, and mean MER = 23 dB.

FIGURE 42

Impulse response at Test Point 7

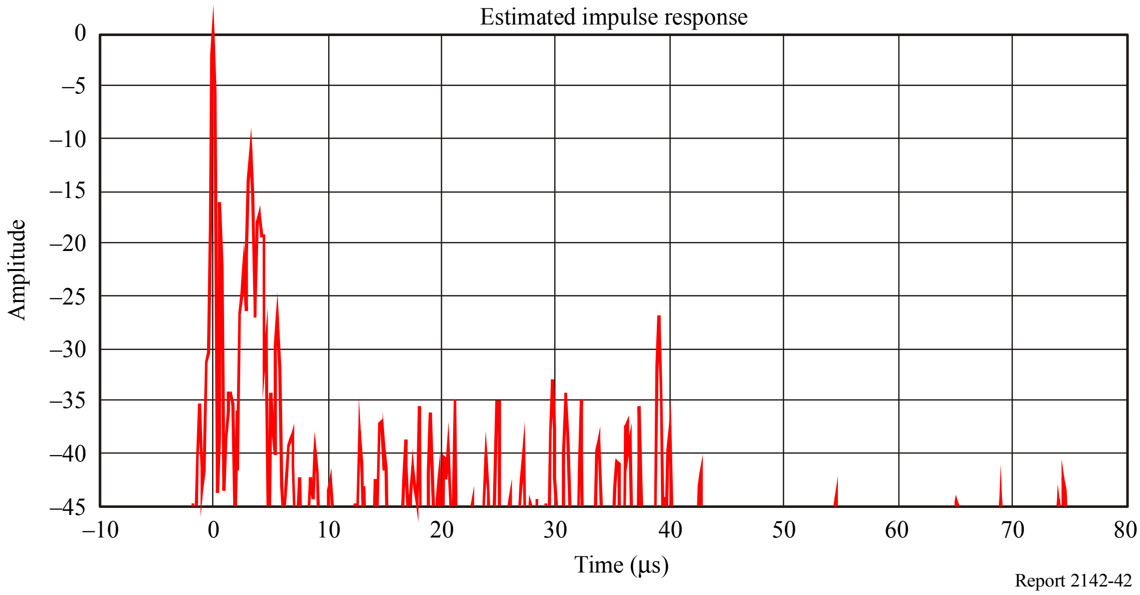

The closest wind turbine is 2.0 km (13 μs delay). The wind turbine in this group furthest from the measuring point (LoS along the ridge) is 3.8 km (24 μs delay). Reflections also occur from a second group of wind turbines. The closest wind turbine in this group is 4.1 km (27 μs delay). The maximum scattering coefficient is –28 dB (–53 dB with an omnidirectional antenna). The multipath signals up to 10 μs are due to terrain scattering near the transmitter, including a very strong multipath signal at 3 μs delay. Mean BER = 0.023, and mean MER = 23 dB.

The following conclusions can be drawn for backscattering:

1 Scattering from individual wind turbines is clearly observed.

2 The excess delay for some turbines (nearest and furthest) was calculated and the results agree well with expectations.

3 The magnitude of the scattered signals varied considerably, but the strongest signal measured was a relatively modest –28 dB (or –53 dB after correcting for the antenna front-to-back ratio). There was not a strong relationship between the signal amplitude and the delay. One explanation is that the wind turbines closest to the measurement point have reflected signals that are well above the height of the measurement antenna.

4 The backscattering from the wind turbines was due almost entirely to the pylons alone, as the wind direction during the measurements resulted in the scattering in different direction from the blades. Thus the measured levels of scattering were largely constant over time. This is in contrast to the forward scattering results below.

3.4.3 Forward scattering case

The measurement of the impulse response in the forward scattering case is difficult, as the multipath excess delays from nearby wind turbines is quite small, often less than the measurement resolution. At the two measurement locations, the scattering angle was small with the wind turbines approximately lying along the path from the transmitter. The direct path from the transmitter was also obscured by a nearby hill, resulting in significant diffraction losses. Measurements and diffraction theory give diffraction losses in the range of 25-30 dB. In the forward scatter measurements, the antenna was pointed at the transmitter, which was also the general direction of scattering from the nearest wind turbines. As the wind turbines were located at the top of the hills, there was a considerable enhancement of the scattered signals relative to the direct signal, and therefore the ratio of the scattered signal to the direct signal was greater than in the backscattering case, despite the actual scattering coefficient being smaller for forward scattering.

The measurements are shown in Figs. 43 and 44. Only the first 10 μs of the impulse response, where the expected scattering occurs, is shown. As the signals are weaker, the cut-off amplitude is –40 dB. Despite the difficulty in resolving the scattered signals, it is clear that there are interference signals for delays less than about 1 μs. The amplitude of this interference from Fig. 44 is plotted as a function of symbol number in Fig. 45, where the variation in the scattered signal as a function of the blade rotation can be observed; the amplitude varies by a factor of 5:1 over a period of about 20 ms. Figures 44 and 45 are from the site detailed in § 3.3.

The delays to the nearest turbines are between 0 and 0.9 μs, with another wind turbine having a delay of 1.6 μs. The scattering from the first group can barely be resolved, but the more distant wind turbine can be observed. The mean MER is 24 dB, and the mean BER is 0.015.

FIGURE 43

Impulse response at Test Point 2

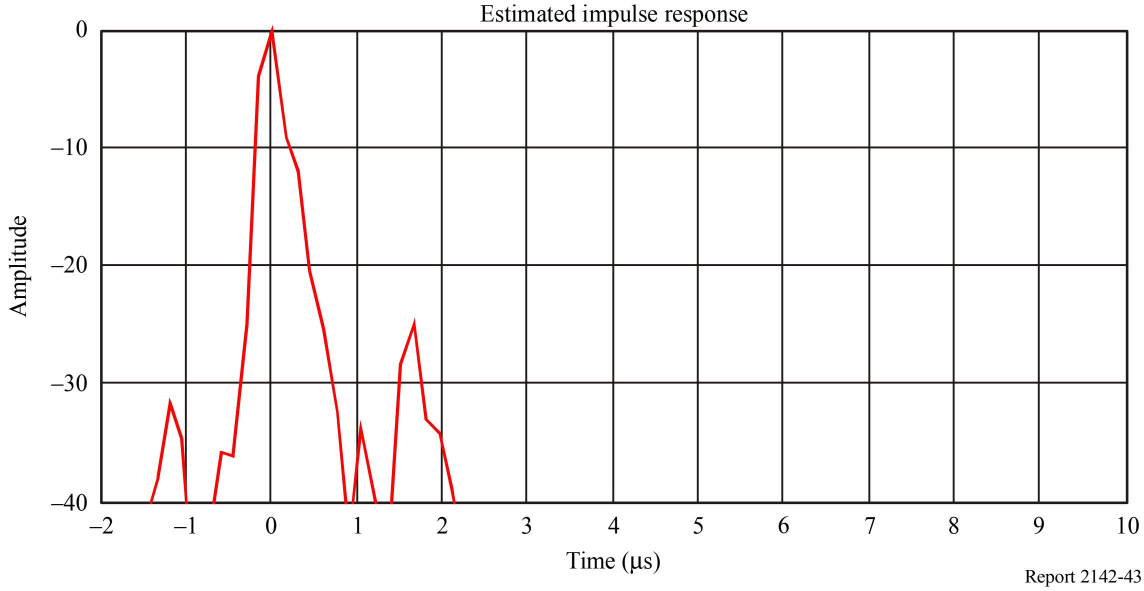

Report 2142-43

FIGURE 44

Impulse response at Test Point 8

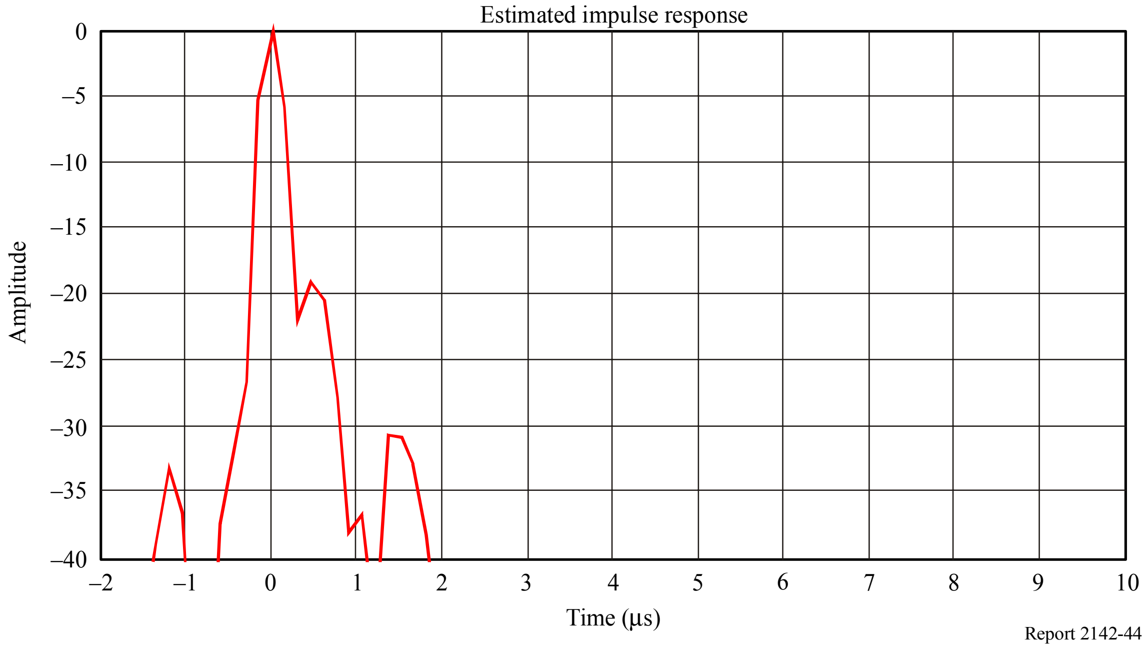

Report 2142-44

As all but one of the wind turbines are nearly on the same line as the direct path to the transmitter, the excess delays are close to zero. The one exception is the wind turbine 1 100 m away (0.5 µs delay). The smaller peak at about 1.5 µs is believed to be the reflections from a row of large trees on the hill with clear LoS to the transmitter. The median MER is 22 dB, and the median BER is 0.028.

FIGURE 45

Scattering at Test Point 8 as a function of symbol number

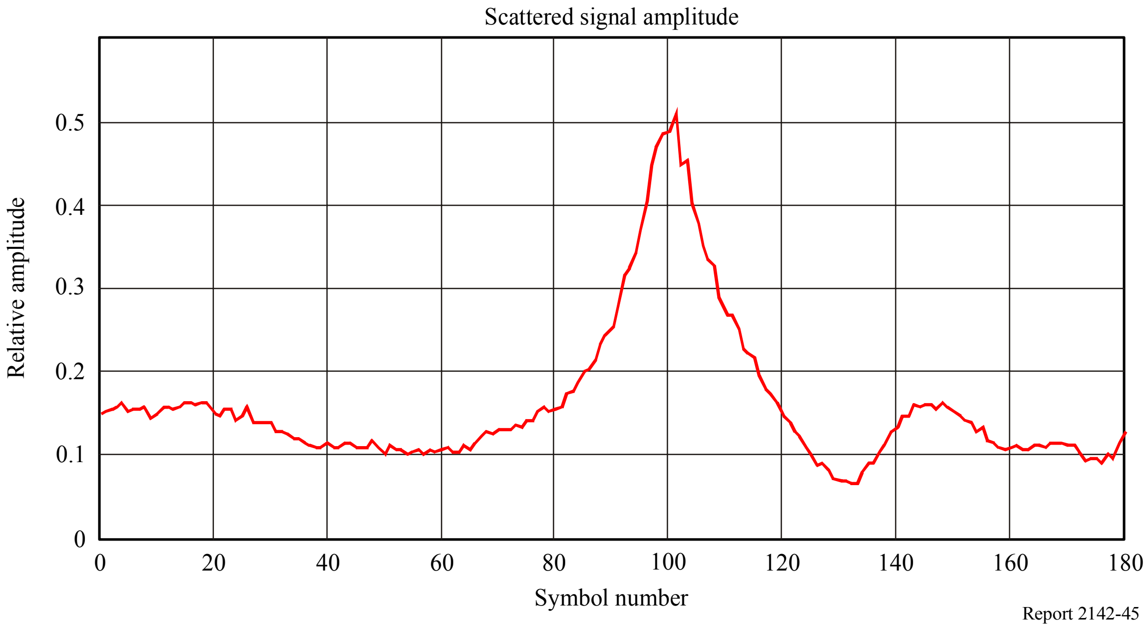

The amplitude variation is due to the rotation of the wind turbine blades.

3.5 Effect of receiving antenna height and ground reflections

Two characteristics of the receiving antenna, directivity and height, are particularly important in determining the quality of the television reception. The effect of directivity was not investigated except as an incidental consequence of the procedure of pointing the antenna at the transmitter (normal situation) or pointing the antenna at the wind farm and away from the transmitter (to enhance the relative strength of the scattered signals). For all measurements in the backscatter region, when the antenna was pointed at the transmitter, there were no observable effects due to the scattering from the wind turbines. This was expected, as the small reflections from the wind turbines were further reduced by the front-to-back ratio of about 25 dB.

However, the effect of height and ground reflections on the received signal strength should be considered. As the ground near the measurement sites was relatively flat and free of obstacles such as trees, it causes reflections which enhance or decrease the received signal relative to the free path signal strength. The effects of ground reflections are shown in Fig. 46 using a two-ray model path gain for a 10-metre receiving antenna. The path gain oscillates as a function of range from the transmitter, so the received signal strength relative to the free path can be as great as +4 dB or as small as –9 dB. Therefore ground reflections can have a significant effect on the received signal.

The parameters used are transmitter height 800 m, receiver height 10 m, surface roughness 10 cm, ground conductivity 0.012 Ω/m, dielectric constant 15.

The reference Test Site 1 is an example where it the two-ray model would be expected to be valid. The range is about 20 km, and the effective transmitter height is about 800 m. Figure 47 shows that the antenna height has a significant effect on the received signal strength. The signal strength does not increase monotonically with height, but has a null at around 6 m. Measurements at the site showed that the signal maximum was at an antenna height of about 10 m. At test site 1, the propagation conditions were such that the signal variation with height did not affect reception quality, but if there is no LoS to the transmitter, it can be significant.

FIGURE 46

Predicted two-ray loss characteristics for path to receiving site

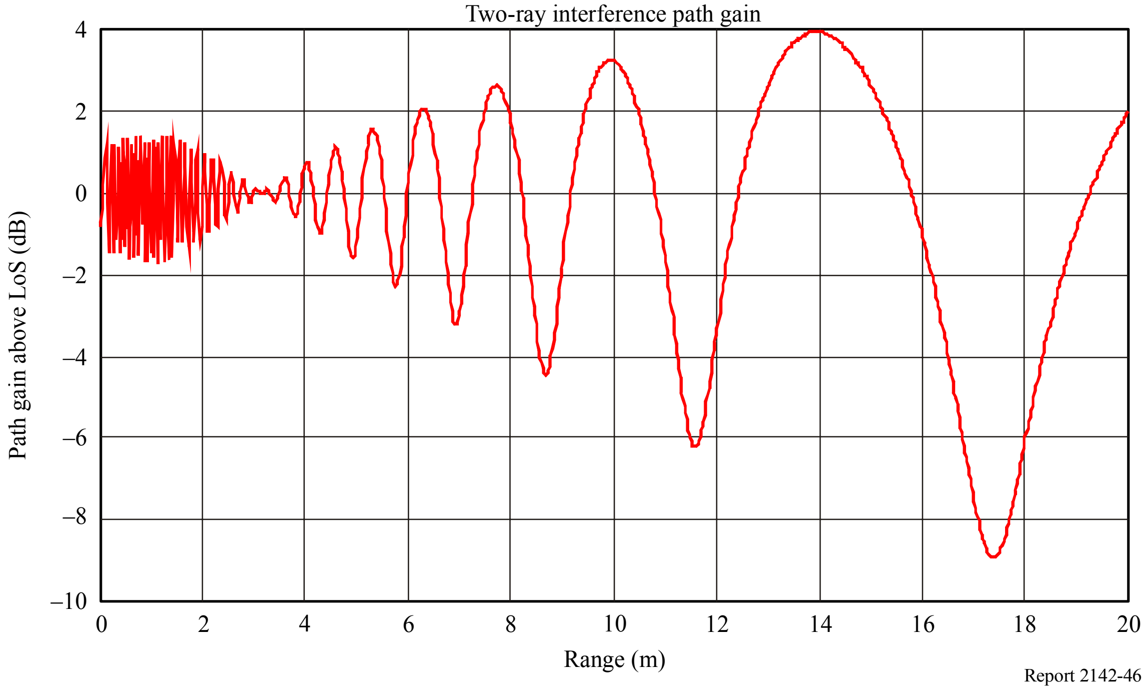

FIGURE 47

Two-ray model predicted path gain as a function of height for Site 1

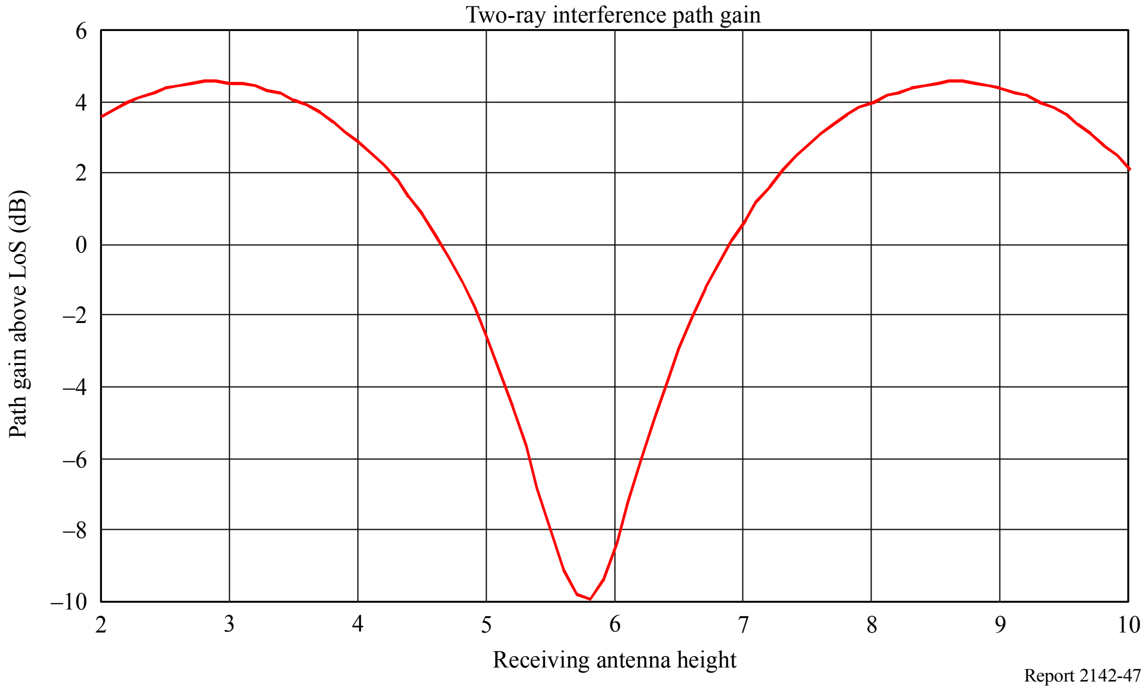

As described in § 3.3, the direct signal at Site 8 is blocked by a nearby hill. The computed effect of ground reflections on both the (diffracted around an adjacent hill) direct signal and the signal scattered from a wind turbine (on top of the hill) is shown in Fig. 48. The ground effect on the scattering from the wind turbine is relatively small, but the effect on the diffracted direct signal is considerable. The initial measurement at Site 8 used an antenna at 10 m height, but none of the digital television receivers could receive the signal. When the antenna height was lowered to 4.5 m (approximately the maximum), the signal was received, though with marginal quality on some receivers. This illustrates the significance of the correct adjustment of antenna height for optimum performance in difficult reception areas. As this was a forward scattering case, antenna gain is of little benefit, in contrast to the backscattering case.

FIGURE 48

Two-ray model predicted path gain as a function of height for Site 8, showing the effect of ground reflections on the direct signal (diffracted over the hill) and the wind turbine on top of the hill

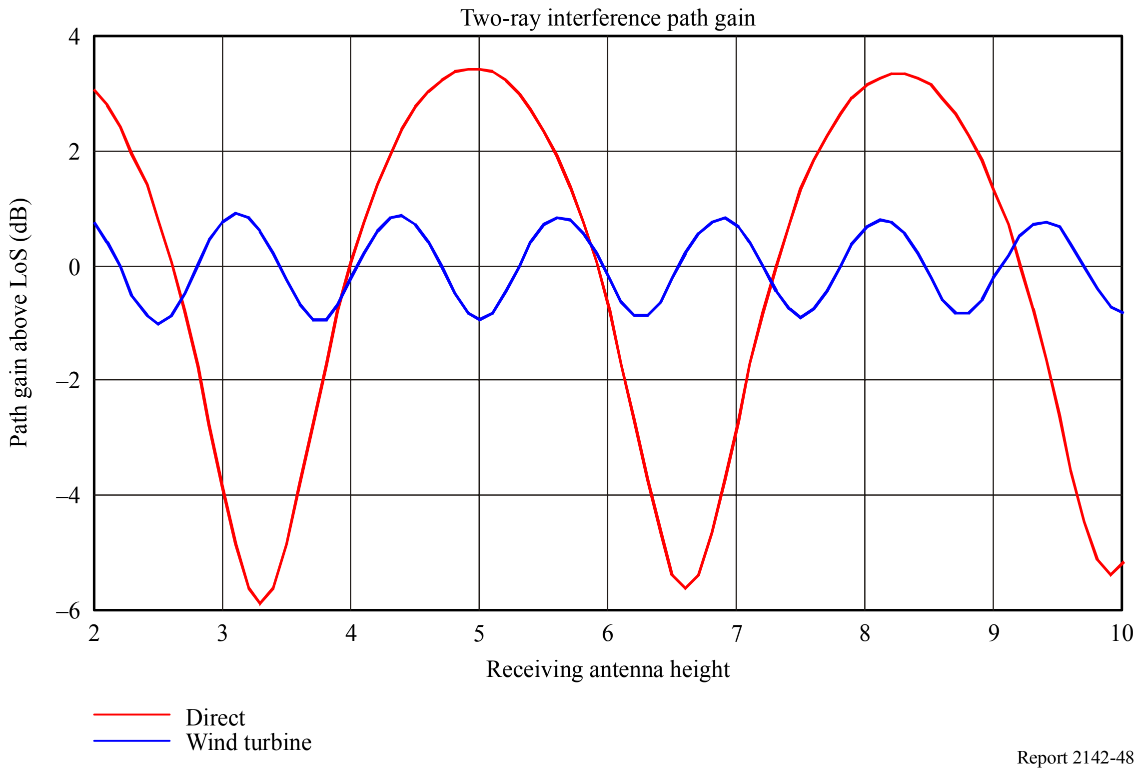

In conclusion, the effect of antenna directivity and ground reflections can have an important effect on the reception of digital television signals. It should not be assumed that increasing the antenna height will improve reception performance. Given the variability of propagation and terrain, installations at difficult reception areas should investigate several positions and heights to find the optimum position.

4 Conclusions

Theory and measurements have investigated the potential for interference to digital television from scattering by wind turbines. Modelling identified the region around a real wind farm where scattering was likely to be greatest, and measurements were then taken in those areas.

For scattering from wind turbines to cause disruption to the reception of digital television, the scattering ratio must exceed a certain threshold determined by the receiver signal processing characteristics. This perceived scattering ratio depends on the scattered signal and the directivity of the receiving antenna. If the interference signals are small a simple antenna will suffice, while with more severe interference a more directive antenna can typically mitigate the interference.

Measurements in the backscatter region, which is largely confined to a narrow region along the line joining the transmitter to the wind farm, using a test antenna of 13 dB gain, resulted in imperceptible interference from the wind turbines. The worst case for backscattering would occur when a hill blocks the direct signal, while clear LoS conditions exist to the wind turbines. In this case, the effective scattering ratio can be severely reduced by 30 dB or more. However, the measurements indicate that even under these extreme conditions it is unlikely that interference will be severe enough to cause disruption to the reception. Therefore for the backscatter case with an appropriate antenna it is unlikely that scattering from wind farms will cause interference.

Measurements in the forward scattering region were prompted by reports that analogue television reception was severely compromised by the presence of the wind turbines; this was confirmed by measurements. The multipath signals from rotating wind turbine blades is very dynamic and was a key interest in this analysis.

The following conclusions can be drawn concerning the dynamic scattering from the blades:

1 Scattering from the blades consists of a slow low amplitude variation at the geometric rotation repetition frequency (one-third the rotation rate) of the blades, as well as a large amplitude but short duration (about 30 ms) interference.

2 The MER measured as a function of time reflects the scattered signal amplitude. As a consequence, the mean value of the MER (as typically measured by instruments) does not reflect the time variations in the MER. The required MER for a receiver operating with interference from a wind turbine was not identified, but observations indicate that the required average MER must be increased above the required minimum of about 20 dB to at least 22 dB to cope with the slowly varying interference. The effect of the rapid, high-amplitude interference was not clear from the limited testing at the wind farm, and further investigations are required to determine the effects on typical receivers.

3 The signal quality as measured on two channels varied considerably. For example, the measured MER on channel 43 (631-638 MHz) was 26 dB, but on channel 37 (589-596 MHz) the MER was 20 dB. The reason for this variability is not clear, but is probably due to the time variation in the signal.

4 The characteristics of the BER before and after the Viterbi decoder are different from the nominal performance specified in Recommendation ITU-R BT.1735. For example, the recommended before-Viterbi BER is 0.04 for an after-Viterbi BER of 2×10^{-4}. However, for the example on channel 43 with a MER of 26 dB, the before-Viterbi BER was 0.021 (well below the recommended threshold), but the after-Viterbi BER was 0.001, well above the suggested level. This characteristic of the error correcting performance is clearly a consequence of the time-variable nature of the interference signal.

In the forward scatter region the antenna pointing towards the transmitter also points towards the wind farm, and the antenna directivity is of little benefit in reducing interference effects. The height of the antenna can be critical, as ground reflections can result in significant signal reduction.

In conclusion, in the backscatter region there is little effect from scattering from wind turbines on the performance of digital television, but in the forward scattering region, if there is significant blockage of the direct signal, significant interference to the reception of the digital television signal is possible. Further study is required to assess the performance of DVB-T receivers operating in the environment of time-varying interference from wind turbines.